K-mouflage Cosmology: the Background Evolution

Philippe Brax, Patrick Valageas

HAL Id: cea-00982376
https://cea.hal.science/cea-00982376

Submitted on 24 Feb 2021

K-mouflage Cosmology: the Background Evolution

Philippe Brax and Patrick Valageas
Institut de Physique Théorique,
CEA, IPhT, F-91191 Gif-sur-Yvette, Cédex, France
CNRS, URA 2306, F-91191 Gif-sur-Yvette, Cédex, France
(Dated: September 3, 2018)

We study the cosmology of K-mouflage theories at the background level. We show that the effects of the scalar field are suppressed at high matter density in the early Universe and only play a role in the late time Universe where the deviations of the Hubble rate from its Λ-CDM counterpart can be of the order five percent for redshifts $1 \lesssim z \lesssim 5$. Similarly, we find that the equation of state can cross the phantom divide in the recent past and even diverge when the effective scalar energy density goes negative and subdominant compared to matter, preserving the positivity of the squared Hubble rate. These features are present in models for which Big Bang Nucleosynthesis is not affected. We analyze the fate of K-mouflage when the nonlinear kinetic terms give rise to ghosts, particle excitations with negative energy. In this case, we find that the K-mouflage theories can only be considered as an effective description of the Universe at low energy below 1 keV. In the safe ghost-free models, we find that the equation of state always diverges in the past and changes significantly by a few percent since $z \lesssim 1$.

I. INTRODUCTION

Scalar fields could be playing a role in late time cosmology and have something to do with the recent acceleration of the expansion of the Universe[1]. They could also induce modifications of gravity on large scales [2] which may be within the reach of the forthcoming EUCLID mission [3]. For instance one always expects at least one scalar field to be present in massive extensions of General Relativity (GR) which could lead to such deviations[4]. In both cases, the mass of the scalar field is very small, implying the possibility of the existence of a scalar fifth force. All in all, scalar fields with low masses acting on very large scales of the Universe are ubiquitous. Nevertheless, such scalars have never manifested themselves in the Solar System or the laboratory where deviations from General Relativity have been painstakingly sought for[5]. It has been recently advocated that this could be the result of the screening of these scalar fields in dense environments[6, 7]. As a result, they would be nearly invisible locally while acting as full fledged modifications of the dynamics of the Universe on large scales.

In this paper, we shall focus on one particular type of screening: K-mouflage[8, 9]. More precisely, we focus on models that have the simplest K-essence form [10], where the nonstandard kinetic term is only a nonlinear function of $(\partial\varphi)^2$. This is a subclass of the possible models that one can build with nonstandard kinetic terms, that may also depend on the field φ or higher derivatives $\partial^2\varphi$ [8]. These models partake in the three types of screening mechanisms which are compatible with second order equations of motion for higher order scalar field theories. In K-mouflage theories, the equations of motion are always second order but the Hamiltonian corresponding to the scalar energy density may be negative for large values of the field's time derivative, depending on the form of

the kinetic term. However, even in such cases, the cosmological screening of the scalar field in high cosmological densities implies that the Hubble rate squared is always positive. Another issue comes from the fact that, when the Hamiltonian becomes negative, the kinetic energy of K-mouflage excitations seen as particles may destabilize the vacuum and lead to a large background of gamma rays. For canonical ghosts, it is known that one cannot extend the validity of the models for energies larger than a few MeV [11]. Here we revisit this issue for K-mouflage models and find that the validity range of these theories is even more restricted to energies always less than 1 keV when ghosts are present. Models where the kinetic term keeps the standard positive sign do not have ghosts and do not suffer from this problem.

A first type of screening which differs from K-mouflage is the chameleon [12, 13](and also the Damour-Polyakov [14]) mechanism. In these models, screened regions are such that the Newtonian potential of dense objects is larger than the value of the scalar field outside the object. A second type of screening is the Vainshtein mechanism [15] which only occurs for noncanonical scalar fields, and where screened regions correspond to a spatial curvature larger than a critical value. The K-mouflage mechanism is also present for noncanonical theories and is effective in regions where the gravitational acceleration is larger than a critical value, in a way reminiscent of the MOND hypothesis [16]. For this reason, K-mouflage models differ from General Relativity on large scales and are well suited to be tested cosmologically. The absence of convergence towards GR in the large distance regime differs drastically from what happens for chameleons. The same lack of convergence is also there for models with the Vainshtein property. On the other hand, the K-mouflage and Vainshtein mechanisms differ locally in the vicinity of a dense object of mass m where the distance below which General Relativity is recovered scales like $m^{1/2}$ and $m^{1/3}$,

respectively. They also differ drastically cosmologically as the latter (Vainshtein) allows for screening of cosmological overdensities like galaxy clusters while the former (K-mouflage) does not screen such large-scale structures. Consequently the theories with the K-mouflage property essentially behave like linear theory with a time dependent Newton constant up to quasilinear scales. In this paper, we will focus on the background evolution and leave the properties of structure formation on large scales for a companion paper [17].

We will concentrate on the cosmology of K-mouflage models and leave their gravitational properties for further work. At the background level and for K-mouflage models leading to the late time acceleration of the expansion of the Universe, we find that the Hubble rate can differ significantly from the one of Λ-CDM for moderate redshifts. This fact corresponds to the cosmological screening at high cosmological densities of the scalar field whose dynamics play a role only when the density of matter is sufficiently small. In the very recent past, the models converge to a Λ-CDM behavior. This implies that the deviations from Λ-CDM are maximal for intermediate redshifts of the order $1 \lesssim z \lesssim 5$. For these redshifts, the effective energy density of the scalar can become positive after being negative in the distant past. This implies in particular that the equation of state is not bounded from below, can be less than -1 and can even diverge. This is an artefact of the the definition of the equation of state with no consequence on the dynamics of the models as the total matter density is always positive. It is remarkable that this result, i.e. the divergence of the equation of state, stands for all models even when the Big Bang Nucleosynthesis constraints [18] on the variation of masses are applied. Moreover, when excluding the possibility of ghosts, the K-mouflage models always cross the phantom divide. A feature which is strikingly different from chameleonlike models [19] and Galileons [20, 21].

In section II, we recall the physical classification of screening models for theories with second order equations of motions. K-mouflage models are particular as screening only occurs when the gravitational acceleration is large enough. In part III, we introduce the K-mouflage models. In section IV, we study the tracking properties of the cosmological background and apply the BBN bounds to K-mouflage. In part V, we study the expansion history of the models and we confirm it numerically in section VI. Finally we study the constraints provided by the gamma ray flux due to ghosts in section VII. We then conclude in section VIII.

II. SCREENING MECHANISMS

A. Background effects

Screening mechanisms can be nicely classified (for a single nearly massless scalar field on very large scales) by considering theories with second order equations of

motion only [22]. In a given environment characterized by overdensities in a sparse background, the scalar field takes a background value, $\varphi_0(t)$, which can be different inside and outside an overdensity. Expanding to second order, the Lagrangian of the fluctuations compared to the background $\delta\varphi = \varphi - \varphi_0(t)$ becomes

$$\mathcal{L} = -\frac{Z(\varphi_0)}{2}(\partial\delta\varphi)^2 - \frac{m^2(\varphi_0)}{2}(\delta\varphi)^2 - \beta(\varphi_0)\frac{\delta\varphi}{M_{\text{Pl}}}\delta\rho_m \quad (1)$$

where $\delta\rho_m$ is the change of the matter density compared to the background. Test particles follow the geodesics of the total potential[29]

$$\Psi = \Psi_{\text{N}} + \beta(\varphi_0)\frac{\delta\varphi}{M_{\text{Pl}}}, \quad (2)$$

where the Newtonian potential Ψ_{N} satisfies the Poisson equation

$$\nabla^2\Psi_{\text{N}} = 4\pi A(\varphi_0)\mathcal{G}_{\text{N}}\delta\rho_{\text{m}} \quad (3)$$

and $\delta\varphi$ is due to the presence of the overdensity. Notice that the true Newtonian constant, as defined from the Poisson equation, is not $\mathcal{G}_{\text{N}} = 1/(8\pi M_{\text{Pl}}^2)$ but $A(\varphi_0)\mathcal{G}_{\text{N}}$ due to the time dependence of the background and the coupling function $A(\varphi)$ characterizing the model. Similarly, we have

$$\beta(\varphi) = M_{\text{Pl}}\frac{\text{d}\ln A(\varphi)}{\text{d}\varphi} \quad (4)$$

for all of these models. The time dependence of Newton's constant has important consequences as it can lead to large modifications of Big Bang Nucleosynthesis (BBN) as well as changes in the orbits of planets and stars which can be constrained using binary pulsars and the Lunar Ranging experiment testing the strong equivalence principle, with a current bound of $|\frac{\dot{\mathcal{G}}_{\text{N}}}{\mathcal{G}_{\text{N}}}| = |\frac{\dot{A}}{A}| \leq 0.2H_0$ [23]. The BBN constraint imposes that the overall variation of particle masses is less than ten percent since BBN [18], i.e $|\frac{\Delta A}{A}| \leq 0.1$ where ΔA is the variation of A. Thus, $A \simeq 1$ in most cosmological configurations in these models.

Screening is defined as a reduction of the effect of the scalar field from the free and linear case of a point particle coupled with a strength $\beta(\varphi_0)$ to matter, i.e. screening occurs when Ψ is smaller than $(1+2\beta^2(\varphi_0))\Psi_{\text{N}}$. Of course this is not equivalent, especially when $\beta(\varphi_0)$ is large, to requiring that the effect of $\beta(\varphi_0)\frac{\delta\varphi}{M_{\text{Pl}}}$ is small compared to Ψ_{N}, which also must be investigated for each experimental situation depending on the appropriate bound on the correction to Ψ_{N}.

B. Chameleon and Damour-Polyakov

Let us focus on theories with $Z(\varphi) = 1$ first, i.e. canonically normalized scalars. At the linear level and in the

quasistatic approximation [19], the equations of motion give that

$$\frac{\delta\varphi}{M_{\text{Pl}}} = -\frac{\beta(\varphi_0)\delta\rho_m}{M_{\text{Pl}}^2\left(m^2(\varphi_0) + \frac{k^2}{a^2}\right)}, \qquad (5)$$

where $k = 1/x$ is the comoving wave number of interest, and

$$\Psi = \left[1 + \frac{2\beta^2(\varphi_0)}{1 + m^2(\varphi_0)a^2/k^2}\right]\Psi_{\text{N}}. \qquad (6)$$

This allows for a direct effect of modified gravity on linear cosmological scales as General Relativity is recovered on very large scales outside the Compton radius, $k/a \lesssim m(\varphi_0)$, and changes to gravity occur inside the Compton radius, $k/a \gtrsim m(\varphi_0)$, with a strength of $(1 + 2\beta^2(\varphi_0))$. When overdensities become greater, the linear approximation is not valid anymore and screening occurs. From Eq.(5) and Poisson's equation (3), in the small-scale linear regime we have $\delta\varphi/M_{\text{Pl}} \simeq 2\beta\Psi_{\text{N}}$. Therefore, the condition for the onset of nonlinear screening, $|\delta\varphi| \sim |\varphi_0|$, can also be written as a condition on the value Ψ_{N} of the Newtonian potential of the object,

$$|2\beta(\varphi_0)\Psi_{\text{N}}| \gtrsim \left|\frac{\varphi_0}{M_{\text{Pl}}}\right|. \qquad (7)$$

Local tests such as the screening of the Milky Way and Solar System experiments impose that the cosmological range of the scalar interaction must be less than 1 Mpc, which implies that most of the cosmological effects of these models are on quasilinear scales. On the other hand, to satisfy the screening condition (7) for objects such as the Earth with $|\Psi_{\oplus}| \sim 10^{-9}$, the field variation in the Milky Way is bounded by $|2\beta M_{\text{Pl}}\Psi_{\oplus}|$, which in turns gives a constraint on the variation of $A(\varphi)$ as

$$\left|\frac{\Delta A}{A}\right| \lesssim \left|\beta(\varphi_0)\frac{\varphi_0}{M_{\text{Pl}}}\right| \le \left|2\beta^2(\varphi_0)\Psi_{\oplus}\right|. \qquad (8)$$

This implies that Newton's constant hardly changed since BBN.

C. K-mouflage and Vainshtein mechanisms

The situation changes for theories with nontrivial kinetic terms. At the linear level and again in the quasistatic approximation, for models dominated by the kinetic term where we can neglect the potential term $m^2(\delta\varphi)^2/2$, we have that

$$\frac{\delta\varphi}{M_{\text{Pl}}} = -\frac{\beta(\varphi_0)a^2\delta\rho_m}{M_{\text{Pl}}^2 Z(\varphi_0)k^2} = \frac{2\beta}{Z}\Psi_{\text{N}}, \qquad (9)$$

and therefore

$$\Psi = \left[1 + \frac{2\beta^2(\varphi_0)}{Z(\varphi_0)}\right]\Psi_{\text{N}}, \qquad (10)$$

and screening occurs when

$$Z(\varphi_0) \gtrsim 1. \qquad (11)$$

Nonlinearly, the modification of gravity around an overdensity is still suppressed when Z is large. We can expand to leading order

$$Z(\varphi) = 1 + a(\varphi)\frac{(\partial\varphi)^2}{\mathcal{M}^4} + b(\varphi)L^2\frac{\Box\varphi}{M_{\text{Pl}}} + \dots, \qquad (12)$$

where $\mathcal{M}$ is a suppression scale characterizing the model, L a typical length scale, and $a(\varphi)$ and $b(\varphi)$ two functions of the order one. Cubic and higher order derivatives are forbidden as they would induce equations of motions of the order larger than two. This implies that this leading order expansion of Z captures the essence of the possible screening mechanisms for theories with second order equations of motion.

1. Vainshtein scenario

When $a = 0$, the suppression of the scalar field effect is due to the Vainshtein effect when the highest derivative in Z satisfies

$$\frac{|\nabla^2\varphi|}{M_{\text{Pl}}} \gtrsim L^{-2}, \qquad (13)$$

implying from Eq.(9) that a necessary condition for screening is

$$|\nabla^2\Psi_{\text{N}}| \gtrsim \frac{|\nabla^2\varphi|}{2\beta M_{\text{Pl}}} \gtrsim \frac{1}{2\beta L^2} \qquad (14)$$

when β is a slowly varying function of φ. Therefore, instead of a criterion on the amplitude of the Newtonian potential itself, as in Eq.(7) for chameleon models, we now have a criterion on its curvature, which also reads as a condition on the density through Poisson's equation, that must be greater than a critical value determined by the length scale L.

Taking the Newtonian potential around a dense object of mass m and understanding the condition (14) in the sense of distribution averaging over a ball of radius r, we find that screening occurs inside the Vainshtein radius [4]

$$R_V = \left(\frac{3\beta L^2 m}{4\pi M_{\text{Pl}}^2}\right)^{1/3}. \qquad (15)$$

For quasilinear cosmological structures, with a density constrast of δ, the Poisson equation reads in the current Universe as

$$\nabla^2\Psi_{\text{N}} = \frac{3}{2}A(\varphi_0)\Omega_{\text{m}}H_0^2\delta, \qquad (16)$$

where Ω_{m0} is the matter density cosmological parameter today. This can lead to screening when

$$3A(\varphi_0)\Omega_{\text{m0}}H_0^2\delta \gtrsim \frac{1}{\beta(\varphi_0)L^2}. \qquad (17)$$

The most interesting models are the ones where the scale L is the size of the current Universe H_0^{-1}. In massive gravity models, this corresponds to a mass of the graviton of the order H_0 and hence effects of modified gravity up to the largest scales. In this case, screening occurs when

$$\delta \gtrsim \frac{1}{3\Omega_{\rm m0} A(\varphi_0)\beta(\varphi_0)}, \tag{18}$$

which is realized for all overdensities with a density contrast larger than a number of the order one as soon as $A(\varphi_0) \sim 1$ from the BBN constraint and $\beta(\varphi_0)$ is not too small (which would render the screening effect irrelevant). Hence all quasilinear structures in the Universe are screened in the Vainshtein models and nonlinear effects must be taken into account even on mildly nonlinear scales.

2. K-mouflage scenario

When $b = 0$, the suppression of the scalar field effect is due to the K-mouflage effect when

$$|\nabla\varphi| \gtrsim \mathcal{M}^2, \tag{19}$$

implying from Eq.(9) that a necessary condition for screening is

$$|\nabla\Psi_{\rm N}| \gtrsim \frac{|\nabla\varphi|}{2\beta M_{\rm Pl}} \gtrsim \frac{\mathcal{M}^2}{2\beta M_{\rm pl}} \tag{20}$$

when β is a slowly varying function of φ. Therefore, instead of a criterion on the amplitude of the gravitational potential, as for chameleon models in Eq.(7), or on its curvature, as for Vainshtein-mechanism models in Eq.(14), we now have a criterion on the gradient of the gravitational potential, that is, the gravitational acceleration.

Taking the Newtonian potential around a dense object of mass m, we find that screening occurs inside the K-mouflage radius [8, 9]

$$R_K = \left(\frac{\beta m}{4\pi M_{\rm Pl}\mathcal{M}^2}\right)^{1/2}. \tag{21}$$

For quasilinear cosmological structures, we find that screening occurs when the wave number k characterizing a given structure satisfies

$$k \lesssim 3\Omega_{\rm m0} A(\varphi_0)\beta(\varphi_0)\frac{H_0^2 M_{\rm Pl}}{\mathcal{M}^2}\delta \tag{22}$$

Taking $\mathcal{M}^4 \sim 3\Omega_{\Lambda 0} M_{\rm Pl}^2 H_0^2$ to recover the acceleration of the Universe now, we have that

$$\frac{k}{H_0} \lesssim \sqrt{\frac{3}{\Omega_{\Lambda 0}}}\Omega_{\rm m0} A(\varphi_0)\beta(\varphi_0)\delta, \tag{23}$$

which corresponds to superhorizon scales if $\delta \sim 1$. As a result, quasilinear objects in the Universe are not screened in K-mouflage models.

For a given scale (such as $x \sim 0.1 - 1h^{-1}$Mpc for large-scale structures and $k = 1/x$), Eq.(23) actually means that only very dense regions, $\delta \gtrsim k/H_0$ are screened. In particular, the condition becomes more severe for smaller scales, in contrast with the scale-independent condition (18) found for the Vainshtein scenario.

In the following we shall concentrate on the background cosmology of K-mouflage. We will find that in the early Universe where densities are large, the effects of the scalar field are screened. The study of the effects of K-mouflage on structure formation is left for a companion paper [17].

III. K-MOUFLAGE

A. Definition of the model

We consider scalar field models where the action in the Einstein frame has the form

$$\begin{aligned} S = &\int {\rm d}^4x \sqrt{-g}\left[\frac{M_{\rm Pl}^2}{2}R + \mathcal{L}_\varphi(\varphi)\right] \\ &+ \int {\rm d}^4x \sqrt{-\tilde{g}}\,\mathcal{L}_{\rm m}(\psi_{\rm m}^{(i)}, \tilde{g}_{\mu\nu}), \end{aligned} \tag{24}$$

where g is the determinant of the metric tensor $g_{\mu\nu}$, and $\psi_{\rm m}^{(i)}$ are various matter fields. The additional scalar field φ is explicitly coupled to matter through the Jordan-frame metric $\tilde{g}_{\mu\nu}$, which is given by the conformal rescaling

$$\tilde{g}_{\mu\nu} = A^2(\varphi)\,g_{\mu\nu}, \tag{25}$$

and $\tilde{g}$ is its determinant. We have already considered various canonical scalar field models in previous works [24, 25], with $\mathcal{L}_\varphi = -(\partial\varphi)^2/2 - V(\varphi)$. In this paper, we consider models with a nonstandard kinetic term

$$\mathcal{L}_\varphi(\varphi) = \mathcal{M}^4 K\left(\frac{X}{\mathcal{M}^4}\right) \quad \text{with} \quad X = -\frac{1}{2}\partial^\mu\varphi\,\partial_\mu\varphi. \tag{26}$$

[We use the signature $(-, +, +, +)$ for the metric.] To focus on the behaviors associated with the nonstandard kinetic term K, we do not add a potential $V(\varphi)$ or a mixed dependence $K(\varphi, X)$ on the field value and the derivative terms. Here, $\mathcal{M}^4$ is an energy scale that will be of the order of the current energy density, (i.e., set by the cosmological constant), to recover the late time accelerated expansion of the Universe. We can choose $\mathcal{M}^4 > 0$ without loss of generality.

It is convenient to introduce the dimensionless variable χ by,

$$\chi = \frac{X}{\mathcal{M}^4} = -\frac{1}{2\mathcal{M}^4}\,\partial^\mu\varphi\partial_\mu\varphi. \tag{27}$$

Then, the canonical behavior [i.e., $K \sim \chi \propto -(\partial\varphi)^2/2$], with a cosmological constant $\rho_\Lambda = \mathcal{M}^4$ [see Eq.(43) below], is recovered at late time in the weak-χ limit if we

have:

$$\chi \to 0 : \quad K(\chi) \simeq -1 + \chi + ..., \qquad (28)$$

where the dots stand for higher order terms. The minus sign of the constant -1 at $\chi = 0$ is set by the condition $\rho_\Lambda = -\mathcal{M}^4 K(0) > 0$, i.e. the corresponding vacuum energy for a uniform configuration should be positive as we have $\mathcal{M}^4 > 0$.

The Klein-Gordon equation that governs the dynamics of the scalar field φ is obtained from the variation of the action (24) with respect to φ. This gives

$$\frac{1}{\sqrt{-g}} \partial_\mu \left[\sqrt{-g} \, \partial^\mu \varphi \, K' \right] - \frac{\mathrm{d} \ln A}{\mathrm{d}\varphi} \, \rho_E = 0, \qquad (29)$$

where $\rho_E = -g^{\mu\nu} T_{\mu\nu}$ is the Einstein-frame matter density, and we note with a prime $K' = \mathrm{d}K/\mathrm{d}\chi$.

B. Positive- and negative-χ tails

From Eq.(27), we can already see that uniform-field configurations have $\chi \geq 0$ whereas (quasi)static configurations have $\chi \leq 0$. Thus, the evolution of the cosmological background, where all fields are uniform, only involves the $\chi \geq 0$ part of the kinetic function $K(\chi)$. As we show in a companion paper, when we consider the formation of cosmological structures (the cosmic web, pancakes, filaments, and clusters of galaxies), we remain rather close to the background value $\bar\chi > 0$. It is only for very dense regions, where $\delta\rho/\bar\rho > ct/r$, that the variable χ can significantly depart from the background value and that we can reach the static limit (e.g., an isolated static field configuration in a Minkowski-like background) where $\chi < 0$. More precisely, we find in the companion paper that on subhorizon scales we can distinguish the two regimes

$$\frac{ctk}{a} \gg 1, \quad \frac{\delta\rho}{\bar\rho} \ll \frac{ctk}{a} : \quad \delta\varphi \text{ is linear}, \qquad (30)$$

and

$$\frac{ctk}{a} \gg 1, \quad \frac{\delta\rho}{\bar\rho} \gtrsim \frac{ctk}{a} : \quad \delta\varphi \text{ is nonlinear}, \qquad (31)$$

for which the fluctuations of the scalar field remain small, i.e.

$$\frac{ctk}{a} \gg 1 : \quad \frac{\delta\varphi}{\bar\varphi} \sim \frac{a^2}{c^2 t^2 k^2} \frac{\delta\rho}{\bar\rho} \ll \frac{\delta\rho}{\bar\rho}, \qquad (32)$$

where $k \equiv 1/x$ is the typical comoving wave number of interest. In Eqs.(30) and (31), "linear" and "nonlinear" denotes whether we can linearize the Klein-Gordon equation (29) around the background value $\bar\varphi$ to obtain the large-scale cosmological fluctuations $\delta\varphi \equiv \varphi - \bar\varphi$ of the scalar field.

For instance, for a typical cluster of galaxies we have $\delta\rho/\bar\rho \sim 200$ and $ct_0/r \sim c/(H_0 r) \sim 3000$ (with $r \sim$

$1h^{-1}\mathrm{Mpc}$), while for the Solar System, up to the Jupiter orbit, we have $\delta\rho/\bar\rho \sim 10^{20}$ and $ct_0/r \sim 10^{14}$. Thus, for large-scale cosmological structures (the cosmic web and clusters) we are in the small-scale (i.e., below the horizon or Hubble radius) and moderate-density regime (30), whereas in the Solar System we are in the small-scale high-density regime (31). Thus, as compared with the mean background density on the size of the Universe, which corresponds to the overall geometry and dynamics of the Universe, structures correspond to both smaller scales and higher densities, and different regimes are reached depending on the relative magnitudes of the relevant density and scale as compared with $\bar\rho$ and c/H_0. Hence moderate-density regions on large scales are described in the linear regime around the background $\bar\chi > 0$. Much denser objects such as the Sun are in the nonlinear regimes where the branch $\chi \leq 0$ must be considered.

In summary, for the cosmological dynamics, both at the level of the background and of the formation of the large-scale structures, we are in the regime associated with $\chi > 0$, whereas the Solar System corresponds to the static regime $\chi < 0$ which is far from the cosmological background. In this paper, we focus on the background cosmological aspects of these modified gravity models. In the companion paper, we also show that the nonlinearities of the kinetic function $K(\chi)$ do not give rise to different scale-dependent qualitative behaviors. Below the horizon, in the regime (30), the modifications of gravity only appear as a time dependent and scale-independent modifications of the equations of motion (e.g., of Newton's constant), with regard to large-scale structure formation. This also means that we do not recover General Relativity on large scales and that the K-mouflage radius is smaller than these cosmological structures. On the other hand, the Solar System corresponds to a different regime where General Relativity may be recovered through the K-mouflage mechanism, depending on the behavior of the kinetic function $K(\chi)$ for large negative χ. This may allow one to build models that are consistent with current Solar System tests of General Relativity.

Because these two regimes are well separated and correspond to different parts of the kinetic function $K(\chi)$, which could behave in unrelated manners if we go beyond polynomials that imply identical power laws at $\pm\infty$, it is convenient to separate the analysis of these two regimes. Thus, we only consider the cosmological part in this paper and the companion paper, and we leave the study of higher-density regions, giving rise to the K-mouflage mechanism, to a future paper.

C. Specific models

For numerical computations we need to specify the kinetic function $K(\chi)$. As noticed above, the evolution of the cosmological background, where all fields are uniform, and of cosmological large-scale structures in the

regime (30), only involve the $\chi \geq 0$ part of the kinetic function $K(\chi)$. Then, as can already be seen from Eq.(29), two different behaviors can be obtained, depending on whether the derivative $K'(\chi)$ has a zero or not on the positive semiaxis. Because of the low-χ behavior (28), which gives $K'(0) = 1$, the case without zero-crossing implies the positive sign, $K' > 0$ for $\chi \geq 0$. As a result, we consider the following three simple examples,

$$\text{"no-}\chi_*, \ K' \geq 1\text{"} \ : \quad K(\chi) = -1 + \chi + K_0\,\chi^m,$$
$$K_0 > 0, \ \ m \geq 2, \qquad (33)$$

$$\text{"with-}\chi_*, \ K' \leq 0\text{"} \ : \quad K(\chi) = -1 + \chi + K_0\,\chi^m,$$
$$K_0 < 0, \ \ m \geq 2, \qquad (34)$$

and

$$\text{"with-}\chi_*, \ K' \geq 0\text{"} : \quad K(\chi) = -1 + \chi - \chi^2 + \chi^3/4. \ (35)$$

The first model (33) corresponds to scenarios where K' never comes across a zero ("no-χ_*") during the background cosmological evolution and remains positive. The second and third models correspond to scenarios where K' comes across a zero ("with-χ_*") at late times (in fact, at infinite time), from below [Eq.(34)] or from above [Eq.(35)], as χ rolls down from $+\infty$. Because the background value of the variable χ always remains above χ_*, in the last two cases it never reaches the low-χ regime (28) and we could have omitted the term -1 [the finite cosmological constant arising from $K(\chi_*)$ instead of $K(0)$].

More generally, the first two terms in Eq.(33), $(-1+\chi)$, represent the first order expansion over χ of a generic function $K(\chi)$, as in Eq.(28), so that we recover a canonical scalar field with a cosmological constant for small time and spatial gradients. The third term $K_0\,\chi^m$ represents the large-χ behavior of the function $K(\chi)$, or more precisely the relevant exponent at the time of interest. For numerical computations, we consider the low order cases $m = 2$ and 3 in models (33) and (34).

For the coupling function $A(\varphi)$, we consider the simple power laws,

$$n \in \mathbb{N}, \ \ n \geq 1 : \quad A(\varphi) = \left(1 + \frac{\beta\varphi}{nM_{\rm Pl}}\right)^n, \qquad (36)$$

which include the linear case $n = 1$, and the exponential limit for $n \to +\infty$,

$$A(\varphi) = e^{\beta\varphi/M_{\rm Pl}}. \qquad (37)$$

Without loss of generality, we normalized the field φ (by the appropriate additive constant) so that $A(0) = 1$.

These forms ensure that $A(\varphi)$ and $K(\chi)$ are always well defined, for all values of the fields. The action (24) is invariant with respect to the transformation $(\varphi, \beta) \to (-\varphi, -\beta)$; therefore we can choose $\beta > 0$. Thus, in addition to the usual cosmological parameters, our system is defined by the five parameters

$$\{\beta, n; K_0, m; \mathcal{M}^4\} \ \text{ with } \ \beta > 0, \ \mathcal{M}^4 > 0, \ n \geq 1, \ m \geq 2, \qquad (38)$$

except for the model (35) where there are no parameters $\{K_0, m\}$ as the kinetic function is fixed. The scale $\mathcal{M}$ is not an independent parameter. For a given value of the set $\{\beta, n; K_0, m\}$ and of H_0, it is fixed by the value of $\Omega_{\rm m0}$ today. Thus, in the numerical computations below, we choose the same set of cosmological parameters today, given by the Planck results [26]. Then, for any set $\{\beta, n; K_0, m\}$, we tune $\mathcal{M}$ to obtain the observed dark energy density today. As noticed above, this means that $\mathcal{M}^4 \sim \bar{\rho}_{\rm de0}$.

IV. COSMOLOGICAL BACKGROUND

A. Equations of motion

We focus on the matter era and we only consider non-relativistic pressureless matter and the scalar field φ. Because the gravitational Lagrangian is not modified in the action (24), the metric $g_{\mu\nu}$ and the Einstein tensor associated with the homogeneous and isotropic background follow the usual FLRW form,

$$g_{\mu\nu} = \text{diag}(-1, a^2, a^2, a^2), \qquad (39)$$

$$G_{00} = 3H^2, \quad G_{ij} = -a^2(2\dot{H} + 3H^2)\delta_{i,j}, \qquad (40)$$

where $a(t)$ is the scale factor, $H(t) = \dot{a}/a$ the Hubble expansion rate, $\delta_{i,j}$ the Kronecker symbol, and $i, j = 1, 2, 3$. Then, the Einstein equations lead to the usual Friedmann equations,

$$3M_{\rm Pl}^2 H^2 \ = \ \bar{\rho}_E + \bar{\rho}_\varphi, \qquad (41)$$
$$-2M_{\rm Pl}^2 \dot{H} \ = \ \bar{\rho}_E + \bar{\rho}_\varphi + \bar{p}_\varphi \qquad (42)$$

where ρ_E, ρ_φ and p_φ, are the matter and scalar field energy densities and pressure (in the Einstein frame). For the Lagrangian (26), the latter read as

$$\bar{\rho}_\varphi = -\mathcal{M}^4\bar{K} + \dot{\bar{\varphi}}^2\,\bar{K}', \quad \bar{p}_\varphi = \mathcal{M}^4\bar{K}. \qquad (43)$$

Here and in the following, the overbar denotes uniform background quantities, and the dimensionless field χ defined in Eq.(27) simplifies as

$$\bar{\chi} = \frac{\dot{\bar{\varphi}}^2}{2\mathcal{M}^4}. \qquad (44)$$

Because the matter Lagrangian involves the rescaled metric $\tilde{g}_{\mu\nu}$, its energy-momentum tensor $T_{\rm (m)}$ is no longer conserved, $D_\mu T_{\rm (m)}^{\mu\nu} \neq 0$, where D_μ is the Einstein-frame covariant derivative. Nevertheless, the Jordan-frame energy-momentum tensor still satisfies the standard conservation law $\tilde{D}_\mu \tilde{T}_{\rm (m)}^{\mu\nu} = 0$. Using Eq.(25), this leads to

$$\dot{\bar{\rho}}_E = -3H\,\bar{\rho}_E + \frac{{\rm d}\ln\bar{A}}{{\rm d}\bar{\varphi}}\,\dot{\bar{\varphi}}\,\bar{\rho}_E, \qquad (45)$$

where we have used the relation $\rho_J = A^{-4}\rho_E$ between the Jordan-frame and Einstein-frame matter densities. It is convenient to introduce the rescaled matter density ρ,

$$\rho = A^{-1}\rho_E, \quad \text{hence} \quad \dot{\bar{\rho}} = -3H\bar{\rho} \quad \text{and} \quad \bar{\rho} = \frac{\bar{\rho}_0}{a^3}, \quad (46)$$

which satisfies the standard conservation equation (and $\bar{\rho}_0$ is the background density $\bar{\rho}$ today).

On the other hand, the Klein-Gordon equation (29) reads as

$$\partial_t\left(a^3\dot{\bar{\varphi}}\bar{K}'\right) = -\frac{\mathrm{d}\bar{A}}{\mathrm{d}\bar{\varphi}}\bar{\rho}a^3, \quad (47)$$

or equivalently

$$\ddot{\bar{\varphi}}\left(\bar{K}' + \frac{\dot{\bar{\varphi}}^2}{\mathcal{M}^4}\bar{K}''\right) + 3H\dot{\bar{\varphi}}\bar{K}' = -\frac{\mathrm{d}\bar{A}}{\mathrm{d}\bar{\varphi}}\bar{\rho}. \quad (48)$$

In particular, this leads to the modified conservation equation

$$\dot{\bar{\rho}}_\varphi = -3H(\bar{\rho}_\varphi + \bar{p}_\varphi) - \frac{\mathrm{d}\bar{A}}{\mathrm{d}\bar{\varphi}}\bar{\rho}\dot{\bar{\varphi}}, \quad (49)$$

where the exchange term between the matter and scalar field compensates as it should the last term of Eq.(45) [because the full energy-momentum tensor must be conserved in the Einstein frame, $D_\mu(T^{\mu\nu}_{(\mathrm{m})} + T^{\mu\nu}_{(\varphi)}) = 0$]. As for the matter sector, it is convenient to introduce an effective scalar field energy density,

$$\rho_\varphi^{\mathrm{eff}} = \rho_\varphi + [A(\varphi) - 1]\rho, \quad (50)$$

which satisfies the standard conservation equation (the pressure p_φ is not modified)

$$\dot{\bar{\rho}}_\varphi^{\mathrm{eff}} = -3H(\bar{\rho}_\varphi^{\mathrm{eff}} + \bar{p}_\varphi). \quad (51)$$

Then, the Friedmann equations (41)-(42) also read as

$$3M_{\mathrm{Pl}}^2 H^2 = \bar{\rho} + \bar{\rho}_\varphi^{\mathrm{eff}}, \quad (52)$$
$$-2M_{\mathrm{Pl}}^2\dot{H} = \bar{\rho} + \bar{\rho}_\varphi^{\mathrm{eff}} + \bar{p}_\varphi, \quad (53)$$

and we define the time dependent cosmological parameters

$$\Omega_{\mathrm{m}} = \frac{\bar{\rho}}{\bar{\rho} + \bar{\rho}_\varphi^{\mathrm{eff}}}, \quad \Omega_\varphi^{\mathrm{eff}} = \frac{\bar{\rho}_\varphi^{\mathrm{eff}}}{\bar{\rho} + \bar{\rho}_\varphi^{\mathrm{eff}}}, \quad w_\varphi^{\mathrm{eff}} = \frac{\bar{p}_\varphi}{\bar{\rho}_\varphi^{\mathrm{eff}}}. \quad (54)$$

B. Recovery of the matter era at early times

To obtain a realistic cosmology, we must check that we recover the usual matter-dominated expansion at early time (we only consider the matter era in this paper), that is, we must have $\bar{\rho}_\varphi^{\mathrm{eff}} \ll \bar{\rho}$ and $\bar{p}_\varphi \ll \bar{\rho}$ as $t \to 0$. From Eq.(50) this implies that $(\bar{A} - 1) \to 0$, hence $\bar{\varphi} \to 0$,

$$t \to 0: \quad \bar{\varphi} \to 0, \quad \bar{A} \simeq 1 + \frac{\beta\bar{\varphi}}{M_{\mathrm{Pl}}}, \quad \frac{\mathrm{d}\bar{A}}{\mathrm{d}\bar{\varphi}} \simeq \frac{\beta}{M_{\mathrm{Pl}}}. \quad (55)$$

Then, the Klein-Gordon equation (47) gives $\dot{\bar{\varphi}}\bar{K}' \to \infty$. We consider models such as (33)-(35) with a power-law behavior at large positive χ, hence

$$t \to 0: \quad \bar{\chi} \to +\infty, \quad \bar{K} \simeq K_0\bar{\chi}^m. \quad (56)$$

[The model (35) has $K_0 = 1/4$ and $m = 3$.] Then, the Klein-Gordon equation (47) can be integrated as

$$t \to 0: \quad a^3\dot{\bar{\varphi}}K_0m\left(\frac{\dot{\bar{\varphi}}^2}{2\mathcal{M}^4}\right)^{m-1} = -\frac{\beta\bar{\rho}_0}{M_{\mathrm{Pl}}}(t + \gamma), \quad (57)$$

where we used the conservation equation (46) and γ is an integration constant. This gives $\dot{\bar{\varphi}} \sim [(t+\gamma)/t^2]^{1/(2m-1)}$, using $a(t) \sim t^{2/3}$, and $\bar{\rho}_\varphi \sim [(t+\gamma)/t^2]^{2m/(2m-1)}$. Requiring that $\bar{\rho}_\varphi \ll \bar{\rho} \sim t^{-2}$ for $t \to 0$ leads to:

$$\gamma = 0 \quad \text{and} \quad m > 1. \quad (58)$$

Therefore, the integration constant γ vanishes and the Klein-Gordon equation (47) can be integrated once to read as

$$t \geq 0: \quad a^3\dot{\bar{\varphi}}\bar{K}' = -\int_0^t \mathrm{d}t'\,\bar{\rho}_0\frac{\mathrm{d}\bar{A}}{\mathrm{d}\bar{\varphi}}(t'). \quad (59)$$

The boundary condition (55), $\bar{\varphi} \to 0$, also implies

$$t \geq 0: \quad \bar{\varphi} = \int_0^t \mathrm{d}t'\,\dot{\bar{\varphi}}(t'). \quad (60)$$

This gives the early time power-law behaviors

$$t \to 0: \quad |\bar{\varphi}| \sim t^{2(m-1)/(2m-1)}, \quad |\dot{\bar{\varphi}}| \sim t^{-1/(2m-1)},$$
$$\bar{\rho}_\varphi^{\mathrm{eff}} \sim \bar{\rho}_\varphi \sim \bar{p}_\varphi \sim t^{-2m/(2m-1)}, \quad (61)$$

and all kinetic models (33)-(35) satisfy $\bar{\rho}_\varphi^{\mathrm{eff}} \ll \bar{\rho}$ at early time, because $m > 1$. Moreover, we have

$$t \to 0: \quad \bar{\rho}_\varphi \sim (2m-1)\mathcal{M}^4\bar{K}, \quad \bar{\rho}_\varphi^{\mathrm{eff}} \sim -\frac{2m-1}{m-1}\mathcal{M}^4\bar{K},$$
$$w_\varphi^{\mathrm{eff}} \simeq -\frac{m-1}{2m-1}. \quad (62)$$

The signs of $\bar{\rho}_\varphi$ and $\bar{\rho}_\varphi^{\mathrm{eff}}$ depend on the sign of K_0. From Eqs.(59)-(60), the signs of $\bar{\varphi}$ and $\dot{\bar{\varphi}}$ are opposite to the sign of K_0 (because $\beta > 0$),

$$t \to 0: \quad K_0\dot{\bar{\varphi}} < 0, \quad K_0\bar{\varphi} < 0. \quad (63)$$

This implies that in the high-density regime of the early Universe, the effects of the scalar field are screened.

C. Classical stability of the background

We discuss here the stability of the early time background solution obtained above when a small perturbation is initially applied. The power-law solution obtained from Eq.(57), with the integration constant $\gamma = 0$, is the

adequate solution of the original Klein-Gordon equation (47), which reads in this regime as

$$\frac{\mathrm{d}}{\mathrm{d}t}\left(a^3\dot{\bar{\varphi}}^{2m-1}\right) = -\frac{\beta}{M_{\mathrm{Pl}}}\bar{\rho}_0\frac{(2\mathcal{M}^4)^{m-1}}{K_0 m}. \qquad (64)$$

If we write the background as $\bar{\varphi} = \bar{\varphi}_0 + \delta\bar{\varphi}$, where $\bar{\varphi}_0$ is the peculiar solution obtained in Sec. IV B, we obtain at linear order

$$\frac{\mathrm{d}}{\mathrm{d}t}\left(a^3\dot{\bar{\varphi}}_0^{2m-2}\delta\dot{\varphi}\right) = 0. \qquad (65)$$

Using the early time power-law behaviors $a \propto t^{2/3}$ and $\dot{\bar{\varphi}}_0 \propto t^{-1/(2m-1)}$, from Eq.(61), this yields

$$\delta\dot{\bar{\varphi}} \sim t^{-2m/(2m-1)}, \quad \delta\bar{\varphi} \sim \text{constant}, \qquad (66)$$

hence

$$\frac{\delta\dot{\bar{\varphi}}}{\dot{\bar{\varphi}}_0} \sim t^{-1}, \quad \frac{\delta\bar{\varphi}}{\bar{\varphi}_0} \sim t^{-2(m-1)/(2m-1)}. \qquad (67)$$

Therefore, the background solution $\bar{\varphi}_0$ obtained in Sec. IV B is stable and is a tracker solution for K-mouflage.

D. Comparison with other modified-gravity scenarios

We can now compare the type of background solution in K-mouflage models and in chameleonlike and Galileon (as an example of the Vainshtein mechanism) models. We have just seen that deviations from Λ-CDM are minimal in the early Universe and at late time for K-mouflage models. The latter requirement is phenomenological and must be imposed to retrieve an equation of state close to -1 since $z \sim 1$. As a result, modifications to the Hubble rate can and do occur for intermediate values of $1 \lesssim z \lesssim 5$. For chameleonlike models, the field tracks the minimum of the effective potential when the mass of the scalar is sufficiently larger than the Hubble rate [19]. In this case the deviations from Λ-CDM are minimal and of order H^2/m^2 which must be always less than 10^{-6} to comply with the absence of deviations from GR in the solar system. Galileons also have a tracker behavior [20], where $\dot{\varphi} \sim H_0^2/H$ and $H^2/H_0^2 = \frac{1}{2}(\Omega_{\mathrm{m}0}a^{-3} + \sqrt{\Omega_{\mathrm{m}0}^2 a^{-6} + 4\Omega_{\Lambda 0}})$ corresponding to an effective time dependent cosmological constant which grows with time. In contrast, $\dot{\varphi}$ and the dark energy density decrease with time in K-mouflage models. This also implies that the departures from the Λ-CDM reference decrease more slowly at higher redshift for the K-mouflage models.

In a similar fashion, in $f(R)$ theories of the form [27] $f(R) = -2\Lambda - f_{R_0}c^2 R_0^{n+1}/(nR^n)$, with $n > 0$ (in the large-curvature regime), the cosmology becomes increasingly close to a Λ-CDM scenario at high redshift. For the K-mouflage scenario, the dark energy component does not converge to a cosmological constant at early times. Thus, w_φ^{eff} goes to a constant that is different from both 0 and -1, see Eq.(62), and the scalar field energy densities $\bar{\rho}_\varphi$ and $\bar{\rho}_\varphi^{\mathrm{eft}}$ actually keep growing, see Eq.(61). Then, we never recover a truly Λ-CDM behavior, with a constant dark energy density, but only the Einstein-de Sitter asymptotics because the dark energy density does not grow as fast as the matter density with redshift.

E. BBN constraint

Particle masses in the Einstein frame are given by

$$m_\psi = A(\varphi)m_\psi^0, \qquad (68)$$

where m_ψ^0 is the bare mass appearing in the Lagrangian. As such, this implies that masses become environmentally dependent. Then, particle masses in the background density have changed since BBN by an amount

$$\frac{\Delta m_\psi}{m_\psi^0} = \Delta\bar{A}. \qquad (69)$$

This corresponds to particles in moderate-density fluctuations, such as Lyman-alpha clouds, filaments, and outer radii of X-ray clusters. The BBN constraint imposes that particle masses must vary by less than $\mathcal{O}(30)\%$ [18] and therefore $|\Delta\bar{A}| \lesssim 1$. High-density regions, where the nonlinear K-mouflage mechanism ensures a convergence to General Relativity through a vanishing of the scalar field gradients, can display a local value φ that differs from the background $\bar{\varphi}$. Therefore, the criterium $|\Delta\bar{A}| \lesssim 1$ may not be sufficient for some models, but it remains a necessary condition.

For the models (36)-(37) that we consider in this paper, the BBN constraint $|\Delta\bar{A}| \lesssim 1$ reads as

$$\left|\frac{\beta\bar{\varphi}}{M_{\mathrm{Pl}}}\right| \lesssim 1, \qquad (70)$$

as $\bar{\varphi} \to 0$ for $t \to 0$.

V. EXPANSION HISTORY

From the integrated form (59) of the Klein-Gordon equation we can see that at late times, in the dark energy era, we have

$$t \to \infty: \quad \dot{\bar{\varphi}}\bar{K}' \to 0. \qquad (71)$$

Therefore, we obtain two different behaviors, depending on whether K' has a zero χ_* on the positive axis, which will set the large-time dynamics, or not, in which case $\dot{\bar{\varphi}}$ and $\bar{\chi}$ go to zero.

A. Expansion history for models with $K' > 0$ for $\chi \geq 0$

We first consider the kinetic models (33) with $K_0 > 0$, or more generally kinetic functions such that $K' > 0$ for $\chi \geq 0$ (i.e., no zero on the positive semiaxis). This implies that $\bar{K}'$ runs from $+\infty$ to 1 as $\bar{\chi}$ rolls down from $+\infty$ to 0 and $\dot{\bar{\varphi}}$ goes from $-\infty$ to 0, following the Klein-Gordon equation (59). We obtain at late times

$$t \to \infty \; : \; \bar{\rho}_\varphi^{\text{eff}} \simeq \mathcal{M}^4, \;\; a(t) \sim e^{\mathcal{M}^2 t/(\sqrt{3} M_{\text{Pl}})},$$
$$\bar{\rho} \propto a^{-3}, \;\; |\dot{\bar{\varphi}}| \sim t \, a^{-3}, \;\; \bar{\varphi} \to \text{constant} < 0, \quad (72)$$

and we recover a cosmological constant behavior, with a constant dark energy density $\bar{\rho}_{\text{de}} = \mathcal{M}^4$.

Because the effective energy density $\bar{\rho}_\varphi^{\text{eff}}$ is negative at early times from Eq.(62), it must change sign and vanish at a time, t_{eff}, before reaching the cosmological constant regime. This implies an effective equation of state parameter w_φ^{eff} that diverges at t_{eff}. To satisfy observational constraints, this time t_{eff} must occur sufficiently far in the past, so that at low redshifts $z \lesssim 1$ where $\bar{\rho}_\varphi^{\text{eff}}$ becomes of the order $\bar{\rho}$ we are close to the cosmological constant regime with $w_\varphi^{\text{eff}} \simeq -1$.

Depending on the value of the parameters K_0 and β, the Universe can go through different regimes. To simplify the analysis, we can use the approximations

$$t_{\text{de}} \sim t_0, \;\; \mathcal{M}^4 \sim \bar{\rho}_0, \;\; a(t) \sim (t/t_0)^{2/3}, \;\; M_{\text{Pl}}^2 \sim \bar{\rho}_0 t_0^2, \quad (73)$$

because the accelerated expansion of the Universe only started at a late time t_{de}, with $z_{\text{de}} \lesssim 1$. Here t_0 is the current age of the Universe. From the BBN constraint (70), we can write $d\bar{A}/d\bar{\varphi} \simeq \beta/M_{\text{Pl}}$. Then, the Klein-Gordon equation (59) and Eq.(60) give $\dot{\bar{\varphi}} \bar{K}' \sim -\beta \bar{\rho} t/M_{\text{Pl}}$ and

$$0 \leq t \leq t_0 : \;\; \frac{\beta \bar{\varphi}}{M_{\text{Pl}}} \sim -\frac{\beta^2}{\bar{K}'}. \quad (74)$$

Thus, the BBN constraint (70) also implies that

$$\left| \frac{\beta^2}{\bar{K}'} \right| \lesssim 1. \quad (75)$$

For large $\bar{\chi}$, where $\bar{K}' \simeq K_0 m \bar{\chi}^m$, the Klein-Gordon equation (59) [i.e., Eq.(57) with $\gamma = 0$] gives

$$t < t_m : \;\; \bar{\chi} \simeq \left(\frac{\beta \bar{\rho} t}{K_0 m M_{\text{Pl}} \sqrt{2\mathcal{M}^4}} \right)^{2/(2m-1)}, \quad (76)$$

whereas at later time, when $\bar{K}' \simeq 1$, we have

$$t > t_m : \;\; \bar{\chi} \simeq \left(\frac{\beta \bar{\rho} t}{M_{\text{Pl}} \sqrt{2\mathcal{M}^4}} \right)^2. \quad (77)$$

The transition time t_m is set by $m K_0 \bar{\chi}^{m-1} = 1$, hence

$$t_m = K_0^{1/[2(m-1)]} \beta \, t_0. \quad (78)$$

[Here and in the following relations, we only look for scalings and orders of magnitude, and we discard irrelevant factors of order unity such as $\sqrt{2}$ or m.] Before this transition time, the scalar field $\bar{\varphi}$ shows the power-law growth (61), and more precisely we obtain:

$$t < t_m : \;\; \frac{\beta \bar{\varphi}}{M_{\text{Pl}}} \sim - \left(\frac{\beta^{2m} t^{2(m-1)}}{K_0 t_0^{2(m-1)}} \right)^{1/(2m-1)}. \quad (79)$$

1. $K_0 \ll 1$

Let us first consider the case of $K_0 \ll 1$. Then, the Universe goes through four stages (we focus on late times after matter-radiation equality):

$$\text{(I):} \;\; t < t_m, \;\; \bar{K} \simeq K_0 \bar{\chi}^m, \;\; \frac{\bar{\rho}_\varphi^{\text{eff}}}{\bar{\rho}} \sim t^{2(m-1)/(2m-1)}, \quad (80)$$

$$\text{(II):} \;\; t_m < t < t_\Lambda, \;\; \bar{K} \simeq \bar{\chi}, \;\; \frac{\bar{\rho}_\varphi^{\text{eff}}}{\bar{\rho}} \simeq \text{constant}, \quad (81)$$

$$\text{(III):} \;\; t_\Lambda < t < t_{\text{de}}, \;\; \bar{K} \simeq -1, \;\; \bar{\rho}_\varphi^{\text{eff}} \simeq \mathcal{M}^4 \ll \bar{\rho}, \quad (82)$$

$$\text{(IV):} \;\; t_{\text{de}} < t, \;\; \bar{K} \simeq -1, \;\; \bar{\rho}_\varphi^{\text{eff}} \simeq \mathcal{M}^4 \gg \bar{\rho}, \quad (83)$$

where we have used the result (61). The first three epochs are distinguished by the regime of the kinetic function $K(\chi)$. The third and fourth epochs, where the scalar field acts as a cosmological constant, are distinguished by the relative importance of the matter and dark energy densities. In practice, as explained above we can take $t_{\text{de}} \sim t_0$. To obtain a Λ-CDM-like behavior, we must also have $t_\Lambda \lesssim t_0$ to recover $w_\varphi^{\text{eff}} \simeq -1$ at late times. This time t_Λ corresponds to $\bar{\chi} = 1$. Using Eq.(77), we obtain

$$K_0 \ll 1 : \;\; t_\Lambda = \beta \, t_0 \;\; \text{hence} \;\; \beta \lesssim 1. \quad (84)$$

The constraint $t_{\text{de}} \simeq t_0$ implies $\mathcal{M}^4 \simeq \bar{\rho}_0$.

From Eqs.(78) and (84), we have in this case the ordering $t_m \ll t_\Lambda \lesssim t_0$. In the time range $t_m < t \leq t_0$, the Klein-Gordon equation (59) gives $\dot{\bar{\varphi}} \sim -\beta \bar{\rho}_0 t_0^2/(M_{\text{Pl}} t) \propto 1/t$. Therefore, neglecting logarithmic corrections, we obtain $\bar{\varphi} \sim \bar{\varphi}(t_m)$ and

$$t_m < t \leq t_0 : \;\; \frac{\beta \bar{\varphi}}{M_{\text{Pl}}} \sim -\beta^2. \quad (85)$$

From the constraint (84), $\beta \lesssim 1$, we can see that the BBN constraint (70) is also satisfied.

For very small K_0, the nonstandard kinetic term $K_0 \chi^m$ only plays a role at early times before the dark energy component takes over. Then, it has no impact on the expansion history of the Universe.

2. $K_0 \gg 1$

Let us now turn to the case of $K_0 \gg 1$. Then, the kinetic term directly shifts from the regime (I) to (III),

that is, from $\bar{K} \simeq K_0 \bar{\chi}^m$ to $\bar{K} \simeq -1$, and we have the sequence

$$\text{(I):} \ \ t < t_\Lambda, \ \bar{K} \simeq K_0 \bar{\chi}^m, \ \frac{\bar{\rho}_\varphi^{\text{eff}}}{\bar{\rho}} \sim t^{2(m-1)/(2m-1)}, \quad (86)$$

$$\text{(II):} \ \ t_\Lambda < t < t_{\text{de}}, \ \bar{K} \simeq -1, \ \bar{\rho}_\varphi^{\text{eff}} \simeq \mathcal{M}^4 \ll \bar{\rho}, \quad (87)$$

$$\text{(III):} \ \ t_{\text{de}} < t, \ \bar{K} \simeq -1, \ \bar{\rho}_\varphi^{\text{eff}} \simeq \mathcal{M}^4 \gg \bar{\rho}. \quad (88)$$

(In other words, we now have $t_m > t_\Lambda$.) The time t_Λ now corresponds to $K_0 \bar{\chi}^m = 1$. This gives

$$K_0 \gg 1: \quad t_\Lambda = K_0^{-1/(2m)} \beta \, t_0 \quad \text{hence} \quad \beta \lesssim K_0^{1/(2m)}. \quad (89)$$

There are two possible orderings for the time t_m which need to be discussed. In the first case, $t_0 < t_m$, $\bar{K}' \simeq m K_0 \bar{\chi}^{m-1}$ until the present time. This corresponds to $K_0^{1/[2(m-1)]} \beta > 1$ from Eq.(78), and we obtain today:

$$K_0^{1/[2(m-1)]} \beta > 1, \ \ t = t_0 \ :$$
$$\bar{K}' \sim \left(\beta^{2m-2} K_0 \right)^{1/(2m-1)} > 1,$$
$$\frac{\beta \bar{\varphi}}{M_{\text{Pl}}} \sim - \left(\frac{\beta^{2m}}{K_0} \right)^{1/(2m-1)} \lesssim 1, \quad (90)$$

where we have used the constraint (89). In the second case, $t_m < t_0$, $\bar{K}' \simeq 1$ today. This corresponds to $K_0^{1/[2(m-1)]} \beta < 1$ and we obtain:

$$K_0^{1/[2(m-1)]} \beta < 1, \ \ t = t_0 \ :$$
$$\bar{K}' \simeq 1, \ \ \frac{\beta \bar{\varphi}}{M_{\text{Pl}}} \sim -\beta^2 \ll 1, \quad (91)$$

where we have used $\beta^2 < K_0^{-1/(m-1)} \ll 1$. Therefore, the BBN constraint (70) is satisfied as soon as the condition (89) is verified. The second case (91), where β is very small, $\beta \lesssim K_0^{-1/[2(m-1)]} \ll 1$, can only give very small deviations from a uniform quintessence model as it yields $|\beta \bar{\varphi}/M_{\text{Pl}}| \ll 1$. Indeed, this implies a coupling function $A(\varphi) \simeq 1$ that is almost constant so that the Einstein-frame and Jordan-frame metrics are almost identical [in scenarios with $\beta \sim 1$, the main effect of the scalar field on the matter geodesics does not arise from the contributions of the fluctuations of ρ_φ to the metric but from the conformal rescaling (25), see the study of the formation of large-scale structures in the companion paper].

3. $K_0 \sim 1$

The case $K_0 \sim 1$ is the transition between the two previous scenarios. We now have:

$$K_0 \sim 1: \quad t_m = t_\Lambda = \beta \, t_0 \quad \text{hence} \quad \beta \lesssim 1, \quad (92)$$

and the Universe goes through three stages as in Eqs.(86)-(88). We also have $\bar{K}' \simeq 1$ today and the condition (92) also implies that the BBN constraint (70) is satisfied.

4. Constraint on β

To summarize the previous results, the constraints associated with a Λ-CDM-like behavior (i.e., $t_\Lambda \lesssim t_0$) and with the BBN condition (70) can be written as

$$\Lambda\text{-CDM-like} + \text{BBN} \Rightarrow \beta \lesssim \max \left[1, K_0^{1/(2m)} \right]. \quad (93)$$

B. Expansion history for models with $K'(\chi_*) = 0$ for some $\chi_* > 0$

We now consider the kinetic models (34) and (35), and more generally kinetic functions such that $K' = 0$ at some positive value $\chi_* > 0$. Then, as χ rolls down from $+\infty$, following the Klein-Gordon equation (59), it will converge at late time to the largest solution χ_* of $K'(\chi_*) = 0$, to obey the asymptotic behavior (71).

1. Models with $K' < 0$ for $\chi > \chi_*$

Let us first discuss the models such as (34), where the derivative K' is negative at large values of χ, to the right of the largest zero χ_*. In the explicit case (34), there is a single critical point χ_*, given by

$$\chi_* = (-mK_0)^{-1/(m-1)}, \quad (94)$$

$$K_* = K(\chi_*) = -1 + \frac{m-1}{m} (-mK_0)^{-1/(m-1)}. \quad (95)$$

To recover a cosmological constant behavior at late time, with $-\bar{p}_\varphi \simeq \bar{\rho}_\varphi \simeq \bar{\rho}_\Lambda > 0$, we must have from Eq.(43) $-\mathcal{M}^4 K_* = \rho_\Lambda > 0$. This implies $K_* < 0$, because $\mathcal{M}^4 > 0$, hence $(-K_0) > (m-1)^{(m-1)}/m^m \sim 1$. Therefore, scenarios with $(-K_0) \ll 1$ are ruled out.

Then, the remaining scenarios have $\bar{K}' < 0$ and $\bar{K} < 0$ at all times. In particular, the effective energy density $\bar{\rho}_\varphi^{\text{eff}}$ is now positive both at late and early times, see Eq.(62). Hence, contrary to the class of models (33), $\bar{\rho}_\varphi^{\text{eff}}$ does not need to change sign and the effective equation of state parameter w_φ^{eff} does not need to diverge at a time t_{eff}. At late times, we recover a cosmological constant behavior, but instead of $\bar{\varphi}$ converging to zero as in Sec. V A, it is $\dot{\varphi}$ that converges to a finite value, and the asymptotics (72) become

$$t \to \infty : \ \bar{\rho}_\varphi^{\text{eff}} \simeq -K_* \mathcal{M}^4, \ a(t) \sim e^{\sqrt{-K_*/3} \mathcal{M}^2 t/M_{\text{Pl}}},$$
$$\bar{\rho} \propto a^{-3}, \ \bar{\varphi} \simeq \sqrt{2\chi_* \mathcal{M}^4} t. \quad (96)$$

Scenarios with $(-K_0) \gg 1$:

Scenarios with $(-K_0) \gg 1$ follow the same expansion history (86)-(88) as those with $K_0 \gg 1$, and the time t_Λ that marks the transition between $\bar{K} \simeq K_0 \bar{\chi}^m$ and $\bar{K} \simeq K_* \simeq -1$ is given by

$$(-K_0) \gg 1: \ t_\Lambda = (-K_0)^{-1/(2m)} \beta \, t_0, \quad (97)$$

hence

$$\beta \lesssim (-K_0)^{1/(2m)}, \qquad (98)$$

in a fashion similar to Eq.(89). Another sign difference is that we now have $\dot{\bar{\varphi}} > 0$ and $\bar{\varphi} > 0$, from Eq.(59), because we now have $\bar{K}' < 0$.

The time t_m, where $\bar{K}'$ shifts from $mK_0\bar{\chi}^{m-1}$ to 1 is still given by Eq.(78), where we take $K_0 \to (-K_0)$. If $t_m > t_0$, which corresponds to $(-K_0)^{1/[2(m-1)]}\beta > 1$, we still have the property (90), with $K_0 \to (-K_0)$,

$$(-K_0)^{1/[2(m-1)]}\beta > 1, \ \ t = t_0 \ :$$
$$\frac{\beta\bar{\varphi}}{M_{\text{Pl}}} \sim \left(\frac{\beta^{2m}}{-K_0}\right)^{1/(2m-1)} \lesssim 1. \ (99)$$

In this case, the linear term χ in Eq.(33) is always subdominant for $t \leq t_0$ and plays no role. If $t_m < t_0$, which corresponds to $(-K_0)^{1/[2(m-1)]}\beta < 1$, the scalar field φ grows linearly with time in the interval $t_m < t < t_0$ and we obtain today

$$(-K_0)^{1/[2(m-1)]}\beta < 1, \ \ t = t_0 \ :$$
$$\frac{\beta\bar{\varphi}}{M_{\text{Pl}}} \sim (-K_0)^{-1/[2(m-1)]}\beta \ll 1.(100)$$

Thus, in both cases the BBN constraint (70) is satisfied

As for the scenario discussed below Eq.(91), the second case (100) only gives very small deviations from a uniform quintessence model as it yields $|\beta\bar{\varphi}/M_{\text{Pl}}| \ll 1$.

Scenarios with $(-K_0) \sim 1$ are allowed if we accept relative deviations from Λ-CDM of order unity. Their scalings can be read from the expressions above where we set $(-K_0) \sim 1$.

2. Models with $K' > 0$ for $\chi > \chi_*$

We now turn to models such as (35), where K' is positive for $\chi > \chi_*$. For the explicit model (35), which has $K_0 = 1/4$ and $m = 3$, the largest zero is

$$\chi_* = 2, \quad K_* = -1. \qquad (101)$$

Because $K_* < 0$ this also corresponds to a positive cosmological constant at late times. As K_0 is of order unity and positive, the expansion history is similar to the one found in Sec. V A 3. That is, we recover the three stages (86)-(88) and the constraint on β is $\beta \lesssim 1$. Because K_0 is positive, as for the models of Sec. V A the effective energy density $\bar{\rho}_{\varphi}^{\text{eff}}$ is negative at early times and it must change sign at a time t_{eff}, where the effective equation of state parameter w_{φ}^{eff} diverges. On the other hand, because of the zero χ_*, φ grows linearly with time as in Eq.(96) at late times, but to negative values as

$$t \to \infty \ : \ \bar{\rho}_{\varphi}^{\text{eff}} \simeq -K_*\mathcal{M}^4, \ \ a(t) \sim e^{\sqrt{-K_*/3}\mathcal{M}^2 t/M_{\text{Pl}}},$$
$$\bar{\rho} \propto a^{-3}, \ \ \bar{\varphi} \simeq -\sqrt{2\chi_*\mathcal{M}^4}t. \qquad (102)$$
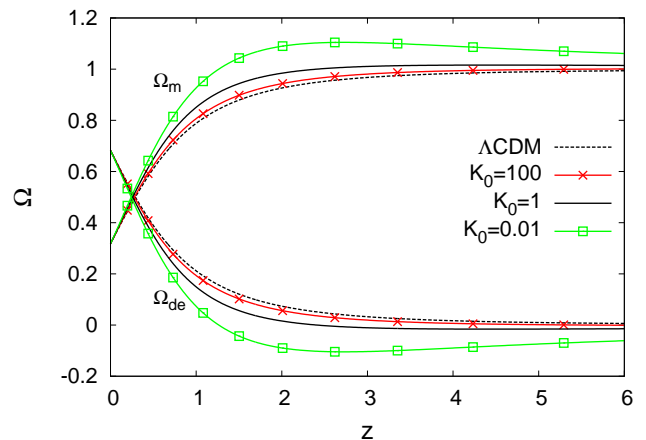

FIG. 1: Evolution with redshift of the matter and dark energy cosmological parameters $\Omega_{\text{m}}(z)$ and $\Omega_{\text{de}}(z)$. The black dashed lines are for the reference Λ-CDM universe and the solid lines are for the scalar field models (33) with different values of K_0 [with $m = 3$, $\beta = 0.3$, and the exponential coupling (37)].

VI. NUMERICAL RESULTS

We compare in this section the evolution with redshift of the background cosmological parameters and of the Hubble expansion rate given by the scalar field models with the reference Λ-CDM Universe. All scenarios have the same background cosmological parameters today, taken from the Planck observations (except of course for the effective dark energy equation of state parameter, w_{φ}^{eff}, which is not exactly equal to -1 for the scalar field models).

A. Models with $K' \neq 0$

We first consider the class of models (33), with the expansion history described in Sec. V A.

1. Dependence on K_0

We consider the density parameters $\Omega_{\text{m}}(z)$ and $\Omega_{\text{de}}(z) = \Omega_{\varphi}^{\text{eff}}(z)$ in Fig. 1. The four scalar field models have the same coupling function parameter $\beta = 0.3$ and exponential form (37), and the same cubic exponent $m = 3$ of the kinetic function (33). They only differ by the value of the kinetic function parameter K_0 (and the derived mass scale $\mathcal{M}$ set to reproduce the current values Ω_{m0} and Ω_{de0}).

We consider three positive values, $K_0 = 100, 1$ and 0.01, to cover the three regimes described in Sec. V A. The curves obtained for larger values of K_0 are closer to the Λ-CDM ones. This agrees with Eqs.(84) and (89), which show that t_{Λ}/t_0 decreases for larger K_0 (especially
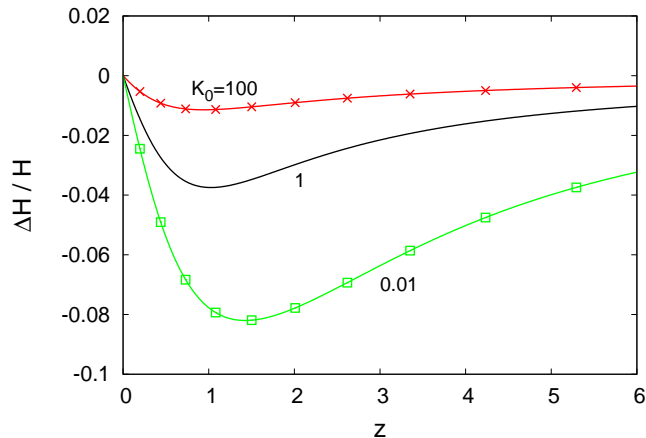
FIG. 2: Relative deviation $[H(z) - H_{\Lambda\text{CDM}}(z)]/H_{\Lambda\text{CDM}}(z)$ of the Hubble expansion rate with respect to the Λ-CDM reference. We consider the same models as in Fig. 1.
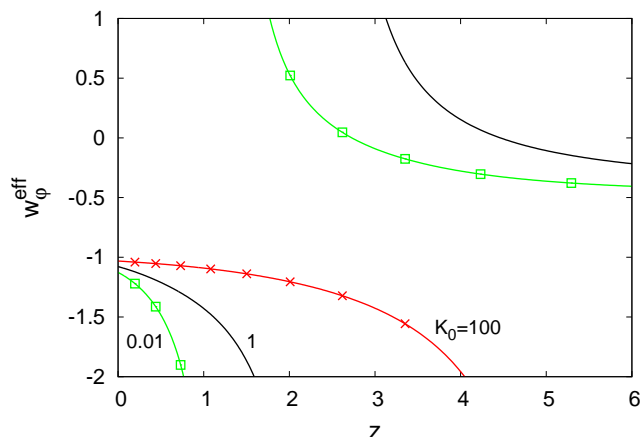

FIG. 4: Scalar field time-derivative term $\bar{\chi}$ of Eq.(44) for the same models as in Fig. 1.

FIG. 3: Effective equation of state parameter w_φ^{eff} for the same models as in Fig. 1.

FIG. 5: Normalized scalar field $\bar{\varphi}/M_{\text{Pl}}$ for the same models as in Fig. 1.

when $K_0 > 1$). Then, when the scalar field energy density becomes relevant (at $t_{\text{de}} \sim t_0$) the kinetic function K is already very close to -1 and it behaves as a cosmological constant. As we noticed below Eq.(72), from Eq.(62), at high redshift the effective scalar field density $\bar{\rho}_\varphi^{\text{eff}}$ is negative. This yields a matter density parameter $\Omega_{\text{m}}(z)$ that is greater than unity and a dark energy density parameter $\Omega_{\text{de}}(z)$ that is negative (we always consider a flat universe).

We consider the same set of models in the following. Thus, we show the Hubble expansion rate in Fig. 2. Again, the behavior is increasingly close to the Λ-CDM reference for larger K_0, at fixed β. Because $\bar{\rho}_\varphi^{\text{eff}}$ is negative at high z if $K_0 > 0$, the Hubble expansion rate is reduced, in agreement with the Friedmann equation (52).

We display the effective equation of state parameter w_φ^{eff} of Eq.(54) in Fig. 3. As explained above, for $K_0 > 0$
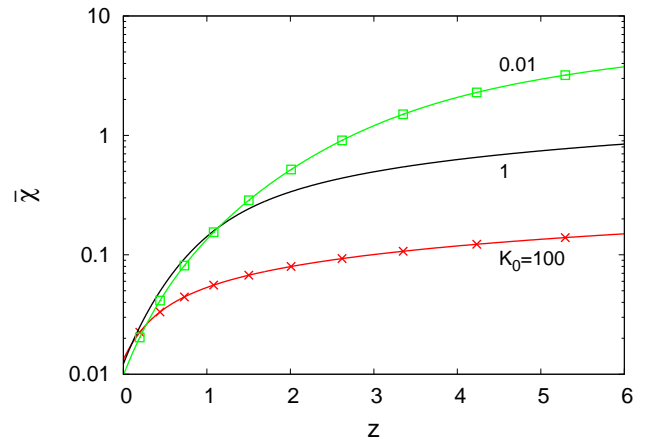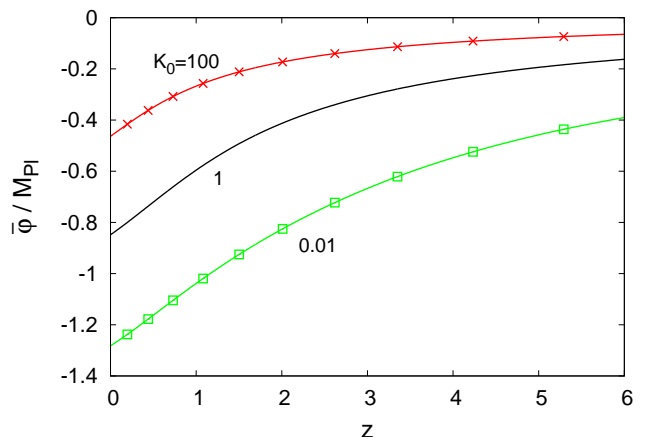
the effective scalar field energy density $\bar{\rho}_\varphi^{\text{eff}}$ is negative at high z, which implies that w_φ^{eff} diverges at some time t_{eff} and also changes sign. In agreement with the previous results and figures, we can check that t_{eff} is pushed farther into the past as K_0 increases, so that over the recent period where $\bar{\rho}_\varphi^{\text{eff}}$ is non-negligible we are increasingly close to $w_\varphi^{\text{eff}} \simeq -1$ and to the Λ-CDM behavior. At high redshift, w_φ^{eff} converges to -0.4 for $m = 3$, see Eq.(62), independently of the other parameters. At $z = 0$ we have $w_\varphi^{\text{eff}} \simeq -1$ because we require being close to the Λ-CDM cosmology. As explained in Sec. V A, this constraint corresponds to an upper bound on β or a lower bound on K_0. In particular, ensuring a value at $z = 2$ of w_φ^{eff} that is sufficiently close to -1 requires a large K_0 (or a small β).

We show the scalar field time-derivative term $\bar{\chi} = \dot{\bar{\varphi}}^2/(2\mathcal{M}^4)$ in Fig. 4 and the normalized scalar field $\bar{\varphi}/M_{\text{Pl}}$
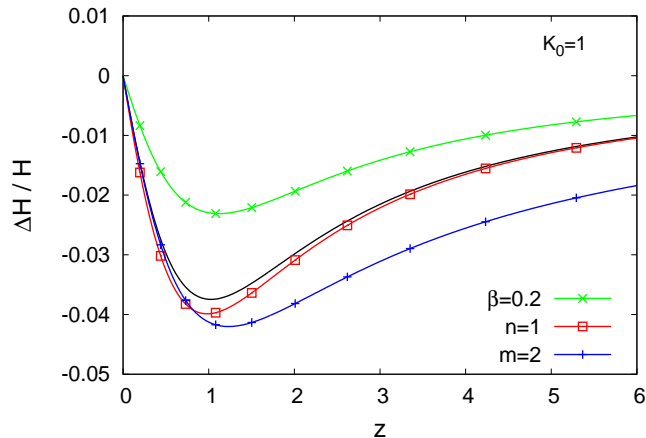
FIG. 6: Relative deviation $[H(z) - H_{\Lambda\text{CDM}}(z)]/H_{\Lambda\text{CDM}}(z)$ of the Hubble expansion rate with respect to the Λ-CDM reference. The solid line is the model $\{\beta = 0.3, n = \infty; K_0 = 1, m = 3\}$ that was also shown in Fig. 2. The lines with symbols are the results obtained when one of these parameters other than K_0 is modified, either $\beta = 0.2$, $n = 1$, or $m = 2$.

FIG. 7: Evolution with redshift of the matter and dark energy cosmological parameters $\Omega_{\text{m}}(z)$ and $\Omega_{\text{de}}(z)$. The black dashed lines are for the reference Λ-CDM universe and the solid lines with symbols are for the scalar field models (34), with $\{\beta = 0.3, n = \infty; K_0 = -5, m = 3\}$ (triangles), and (35) (crosses).

in Fig. 5. The amplitude of the scalar field and of its time derivative decrease for larger K_0, in agreement with the previous results. As seen in Sec. V, the squared time derivative $\bar{\chi}$ goes to zero at late time while $\bar{\varphi}$ converges to a finite value, see Eq.(72). In agreement with Eq.(63), we can check that $\bar{\varphi}$ and K_0 are of opposite signs.

The fact that χ grows at early time, even though $\bar{\varphi}$ goes to zero, means that the energy density $\bar{\rho}_\varphi^{\text{eff}}$ also grows, as $t^{-2m/(2m-1)}$ as seen in Eq.(61). Therefore, the dark energy component becomes subdominant in the past at a slower rate than a cosmological constant. This leads to the slow decrease with redshift of the deviation from the Λ-CDM reference seen in Figs. 1 and 2. This means that moderate redshifts, up to $z \lesssim 3$, contain significant information on the underlying model in this class of scenarios.

2. Dependence on β, n, and m

We show in Fig. 6 the dependence of the Hubble expansion rate on other parameters of the scalar field model than K_0. Taking for reference the case $\{\beta = 0.3, n = \infty; K_0 = 1, m = 3\}$ that was also displayed in Figs. 1-5, we show the results we obtain when we modify one of these other parameters.

Going from the exponential form (37) (i.e., $n = \infty$) to the linear form (36) ($n = 1$) makes very little change. This agrees with the fact that we require $|\beta\bar{\varphi}/M_{\text{Pl}}| \lesssim 1$ to comply with the BBN constraint (70), which means that the coupling function $A(\varphi)$ is well approximated by its first order expansion $\bar{A} \simeq 1 + \beta\bar{\varphi}/M_{\text{Pl}}$ and the higher order terms, which depend on n, can be neglected when we look for $H(z)$.

Modifying the exponent m of the large-χ power-law

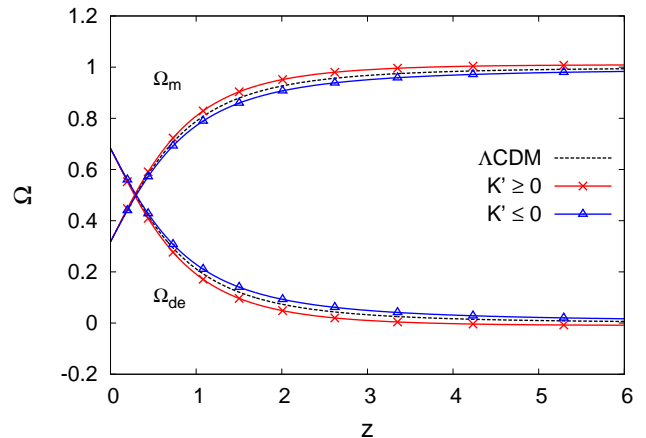behavior of the kinetic function $K(\chi)$, from $m = 3$ to $m = 2$, makes a quantitative change of about 1% for $H(z)$, but as expected the qualitative shape is not modified.

The main dependence comes from the amplitude β of the coupling function $\bar{A} \simeq 1 + \beta\bar{\varphi}/M_{\text{Pl}}$. Indeed, at late times $\bar{K}' \simeq 1$ [unless K_0 is very large, as in Eq.(90)], and the main combination that describes the deviation from Λ-CDM is $\beta\bar{\varphi}/M_{\text{Pl}} \sim -\beta^2$, see Eq.(74). Therefore, the amplitude of the deviation from Λ-CDM is mostly controlled by β^2 and it grows with β^2, as we can check in Fig. 6.

B. Models with a fixed point, $K'(\chi_*) = 0$

We now consider the classes of models (34)-(35), with the expansion history described in Sec. V B.

We consider the density parameters $\Omega_{\text{m}}(z)$ and $\Omega_{\text{de}}(z)$ in Fig. 7. For the model (35), where $\bar{K}' > 0$, we obtain results that are similar to those obtained in Fig. 7, because at early times it belongs to the same class with $K_0 > 0$. Thus, the effective scalar field density $\bar{\rho}_\varphi^{\text{eff}}$ is negative at early times, which yields a matter density parameter, $\Omega_{\text{m}}(z)$, that is greater than unity and a dark energy density parameter, $\Omega_{\text{de}}(z)$, that is negative.

For the model (34), where $\bar{K}' < 0$, the effective scalar field density $\bar{\rho}_\varphi^{\text{eff}}$ is always positive, which leads to a matter density parameter, $\Omega_{\text{m}}(z)$, that is smaller than unity and a dark energy density parameter, $\Omega_{\text{de}}(z)$, that is positive, as in the Λ-CDM scenario. In fact, in terms of Ω_{m} and Ω_{de}, the deviation from Λ-CDM is of the opposite sign compared to the one obtained in the case of $K_0 > 0$.

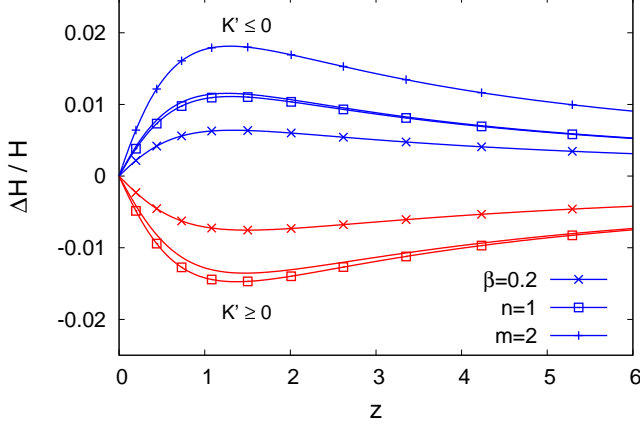We show the Hubble expansion rate in Fig. 8, for these two reference models and their variants when we modify

FIG. 8: Relative deviation $[H(z) - H_{\Lambda\mathrm{CDM}}(z)]/H_{\Lambda\mathrm{CDM}}(z)$ of the Hubble expansion rate with respect to the Λ-CDM reference. We consider the same two reference models as in Fig. 7, together with their variants when we modify either β, n, or m [only for the case of (34)].
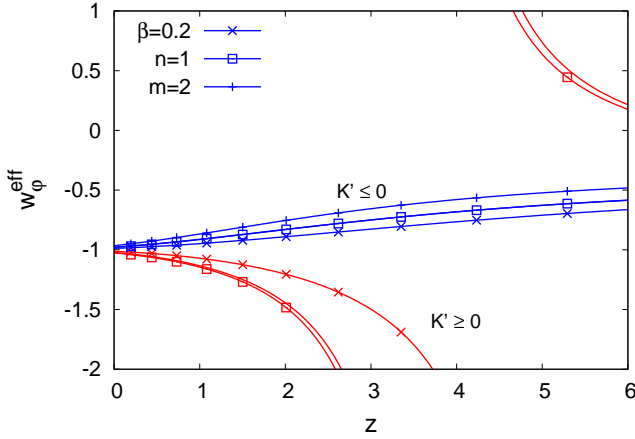

FIG. 10: Scalar field time-derivative term $\bar{\chi}$ of Eq.(44) for the same models as in Fig. 8.

FIG. 9: Effective equation of state parameter w_φ^{eff} for the same models as in Fig. 8.

FIG. 11: Normalized scalar field $\bar{\varphi}/M_{\mathrm{Pl}}$ for the same models as in Fig. 8.

either β, n, or m [only for the case of (34) because the model (35) has a fixed $m = 3$]. As for the cosmological parameters $\Omega_{\mathrm{m}}(z)$ and $\Omega_{\mathrm{de}}(z)$ shown in Fig. 7, the change of sign of K_0 corresponds to a change of sign in the deviation of the Hubble expansion rate from the Λ-CDM reference. Indeed, because $\bar{\rho}_\varphi^{\mathrm{eff}}$ is negative at high z if $K_0 > 0$, the Hubble expansion rate is reduced, in agreement with the Friedmann equation (52). In contrast, if $K_0 < 0$, $\bar{\rho}_\varphi^{\mathrm{eff}}$ is positive at high z and grows with redshift, see Eq.(61) (whereas in the Λ-CDM scenario ρ_Λ is constant), so that the Hubble expansion rate is greater. Again, the model (35) gives results that are similar to those obtained in Fig. 2 for the class (33), because they belong to the same category at high redshift.

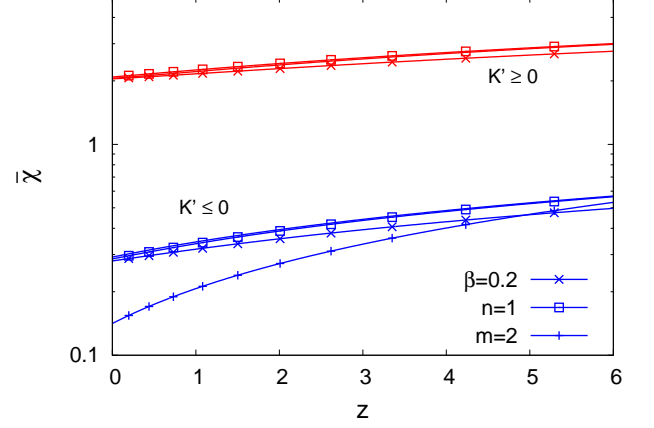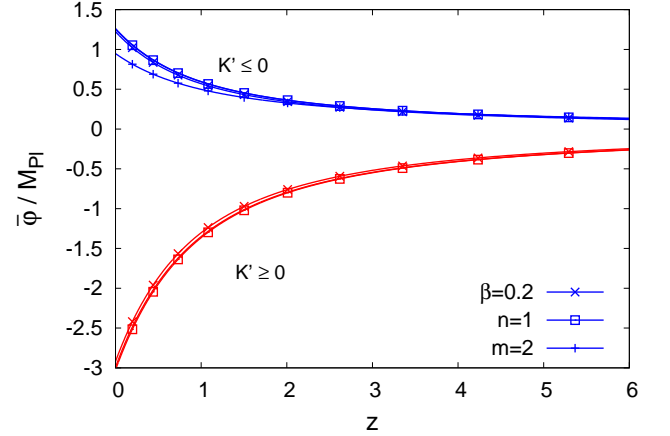We display the effective equation of state parameter w_φ^{eff} of Eq.(54) in Fig. 9. As explained above, for $K_0 > 0$ the effective scalar field energy density $\bar{\rho}_\varphi^{\mathrm{eff}}$ is negative at high z, which implies that w_φ^{eff} diverges at some time t_{eff} and also changes sign. Thus, for the class of models (35) we recover the behavior found in Fig. 3. For the class of models (34), where $K_0 < 0$, the effective scalar field energy density $\bar{\rho}_\varphi^{\mathrm{eff}}$ is always positive and w_φ^{eff} smoothly runs with time from $-(m-1)/(2m-1)$ to -1. This also means that models with $K_0 \lesssim -1$ are very close to the Λ-CDM reference, with respect to such background quantities, because w_φ^{eff} does not go very far from -1, whereas models with $K_0 > 0$ have an equation of state parameter w_φ^{eff} that goes through $\pm\infty$ and to ensure a value at $z = 2$ that is sufficiently close to -1 requires a large K_0 (or a small β).

We show the scalar field time-derivative term $\bar{\chi} = \dot{\bar{\varphi}}^2/(2\mathcal{M}^4)$ in Fig. 10 and the normalized scalar field
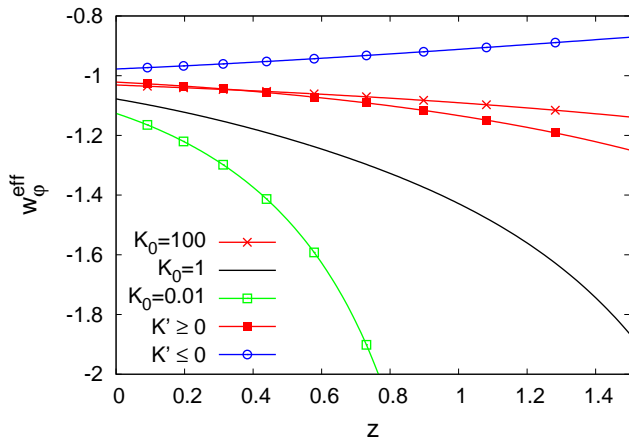
FIG. 12: Effective equation of state parameter w_φ^{eff} for the same models as in Figs. 1 and 7.

$\bar{\varphi}/M_{\text{Pl}}$ in Fig. 11. Contrary to the models (33) considered in Sec. VI A, at late times the squared time-derivative $\bar{\chi}$ goes to a nonzero value χ_* and $\bar{\varphi}$ keeps growing linearly with time, in agreement with Eqs.(96) and (102). The sign of $\bar{\varphi}$ is opposite to the one of K_0 (or more generally $\bar{K}'$).

C.   Equation of state w_φ^{eff}

We summarize in Fig. 12 our results for the various models studied in this paper in terms of the effective equation of state parameter $w_\varphi^{\text{eff}}(z)$ at low redshift. This shows the variety of behaviors that can be obtained within this class of K-mouflage scenarios.

VII.   GHOSTS AND K-MOUFLAGE

The K-mouflage theories that we have considered so far have second order equations of motions. We have seen that their cosmological solutions are classically stable. On the other hand, they can have ghost instabilities when the kinetic energy becomes negative, as in the class of models (34) with $K_0 < 0$. Because we have specified that the models have a positive sign for the kinetic energy when χ is small, see Eq.(28), this can only happen when χ is large or beyond the largest zero χ_* of $K'(\chi)$, where the dynamics are dominated by the higher order terms in the kinetic function $K(\chi)$.

We have already seen that the appearance of negative energies for the effective scalar field energy density $\bar{\rho}_\varphi^{\text{eff}}$ in the past implies that the effective equation of state w_φ^{eff} crosses the phantom divide and even diverges for a redshift which is $z \gtrsim 1$. This is not a serious problem for the models as the total energy density including matter is always positive. Nonetheless, this puts some constraints on

parameters such as $K(0) < 0$ for the class of models (33) and $K(\chi_*) < 0$ for the classes of models (34) and (35). The positivity condition, which ensures that $H^2 > 0$, is automatically satisfied at early times when $m > 1$ because the scalar field becomes subdominant, as described in Sec. IV B. The condition $m > 1$ shows that this behavior can be ascribed to the effective screening of the K-mouflage field at high cosmological density, because it relies on the nonlinearity of the kinetic function $K(\chi)$. Note that the crossing of the phantom divide, associated with $\bar{\rho}_\varphi^{\text{eff}} < 0$ at early times, actually corresponds to positive scalar field density, $\bar{\rho}_\varphi > 0$, and positive K_0, see Eq.(62). This change of sign is due to the factor $(\bar{A}-1)\bar{\rho}$ in Eq.(50), which happens to be of the opposite sign and with a slightly larger amplitude than $\bar{\rho}_\varphi$ in this regime.

Here we shall investigate the quantum instability of the vacuum due to the existence of states with negative energies [11]. This corresponds to the models of the class (34) where there is no crossing of the phantom divide, $w_\varphi^{\text{eff}} > -1$. This can be conveniently analyzed by expanding the Lagrangian around the cosmological background, $\varphi = \bar{\varphi} + \delta\varphi$. This defines an effective field theory for the quantum field $\delta\varphi$, and introducing

$$\delta\chi \equiv \chi - \bar{\chi} = \frac{1}{2\mathcal{M}^4} \left[2\dot{\bar{\varphi}}\frac{\partial\delta\varphi}{\partial t} + \left(\frac{\partial\delta\varphi}{\partial t}\right)^2 - \sum_{i=1}^{3}\left(\frac{\partial\delta\varphi}{\partial x_i}\right)^2 \right] \tag{103}$$

we obtain from Eq.(26) the Lagrangian

$$\mathcal{L}_{\delta\varphi} = \mathcal{M}^4 \sum_{\ell=1}^{\infty} \frac{\bar{K}^{(\ell)}}{\ell!}(\delta\chi)^\ell, \tag{104}$$

where $\bar{K}^{(\ell)} = \frac{\mathrm{d}^\ell K}{\mathrm{d}\chi^\ell}(\bar{\chi})$. If the power m is an integer, or more generally if $K(\chi)$ is a polynomial of the order m, the series (104) terminates and it only contains m terms, $\ell \leq m$. The time dependent cosmological background breaks the Lorentz invariance for the field $\delta\varphi$, and the lowest order term reads as

$$\mathcal{L}_{\delta\varphi}^{(2)} = \left(\frac{\bar{K}'}{2} + \bar{\chi}\bar{K}''\right)\left(\frac{\partial\delta\varphi}{\partial t}\right)^2 - \frac{\bar{K}'}{2}\sum_{i=1}^{3}\left(\frac{\partial\delta\varphi}{\partial x_i}\right)^2. \tag{105}$$

For the models (33) and (35), $\bar{K}'$ and $\bar{K}''$ are positive and the kinetic term (105) has the standard sign. There is no ghost but the field $\delta\varphi$ propagates at a speed, $c_{\delta\varphi}$, that is smaller than the speed of light,

$$c_{\delta\varphi}^2 = \frac{\bar{K}'}{\bar{K}' + 2\bar{\chi}\bar{K}''} c^2 < c^2. \tag{106}$$

For the models (34), with $K_0 < 0$ and $m > 1$, $\bar{K}'$ and $\bar{K}''$ are negative and the kinetic term (105) has a nonstandard negative sign. The propagation speed is again smaller than light and given by Eq.(106), but now there are ghost instabilities. Because of the negative sign, the propagator of this theory for the quantum field $\delta\varphi$ propagates negative energy states. These negative energy

states destabilize the vacuum as positive energy particles can be created from nothing, being compensated by the appearance of ghosts to preserve the conservation of energy. In this case, the vacuum becomes unstable and the background radiation of those particles created from the vacuum should be observed. Applying bounds on the spectrum of gamma rays in the Universe leads to constraints on the highest energies available to the created particles, i.e. the cutoff energy of the model.

It is convenient to normalize the ghost field as $\delta\varphi = \phi/\sqrt{-\bar{K}' - 2\bar{\chi}\bar{K}''}$. The higher order terms in the Lagrangian are treated as perturbative self-interactions of the scalar field and also involve interactions between the scalar and the graviton. They contain terms of the form

$$\mathcal{L}_\phi^{(2\ell)} \supset \frac{\bar{K}^{(\ell)}}{2^\ell \ell! \mathcal{M}^{4(\ell-1)} |\bar{K}' + 2\bar{\chi}\bar{K}''|^\ell} [-(\partial\phi)^2]^\ell. \quad (107)$$

For the models considered in Sec. III C, where $\bar{\chi} \sim t^{-2/(2m-1)}$ at early times from Eq.(61), this gives terms of the form $[-(\partial\phi)^2]^\ell/M^{4(\ell-1)}$, with a time dependent mass

$$M \sim \mathcal{M} (t/t_0)^{-m/[2(2m-1)]}. \quad (108)$$

This mass grows at early times because of the nonlinearity of the kinetic function $K(\chi)$, associated with the K-mouflage mechanism. This comes from the increasing kinetic prefactor in Eq.(105) and implies that it is more difficult to create ghosts in the past. These terms give rise to a linear coupling between the graviton and the ghost of the form

$$\mathcal{L}^{(2\ell)} \supset \frac{h_{\mu\nu}}{M_{\mathrm{Pl}}} \frac{\partial^\mu \phi \partial^\nu \phi (\partial\phi)^{2(\ell-1)}}{M^{4(\ell-1)}}, \quad (109)$$

(where $h_{\mu\nu} = M_{\mathrm{Pl}} \delta g_{\mu\nu}$) which corresponds to a vertex with 2ℓ momenta and $2\ell + 1$ particles. Taking into account the vertex between one graviton and two photons of the type (we only pick one part)

$$\mathcal{L}_\gamma = \frac{h_{\mu\nu}}{M_{\mathrm{Pl}}} \partial^\mu A^\rho \partial^\nu A_\rho, \quad (110)$$

we can draw a vacuum diagram containing the (2ℓ) ghosts and two photons created from a graviton fluctuation from the vacuum. This diagram is obviously kinematically forbidden when the scalars are not ghosts. Here on the contrary the two photons with positive energies appear at the same time as scalars with negative energies. The creation rate is given by

$$\Gamma_{(2\ell)} = \int \frac{d^4 p}{(2\pi)^4} (\prod_{i=1}^{2\ell} \frac{d^3 p_i}{(2\pi)^3 2E_i}) (\prod_{j=1}^{2} \frac{d^3 p'_j}{(2\pi)^3 2E'_j})$$

$$\times (2\pi)^4 \delta^{(4)}(p - p'_1 - p'_2)(2\pi)^4 \delta^{(4)}(p - \sum_{i=1}^{2\ell} p_i) |\mathcal{M}_{(2\ell)}|^2$$

$$(111)$$

where the matrix element is symbolically

$$\mathcal{M}_{(2\ell)} \sim \frac{(\prod_{i=1}^{2\ell} p_i) p'_1 p'_2}{M_{\mathrm{Pl}}^2 M^{4(\ell-1)} p^2}, \quad (112)$$

i.e. one momentum appears for each scalar and each photon, and there is one graviton propagator. Notice that the dispersion relation for the ghosts is now $E^2 = c_{\delta\varphi}^2 p^2$. Cosmologically, Lorentz invariance is broken and we consider the K-mouflage models to be effective field theories with an explicit cutoff Λ. This cutoff would correspond to the highest energies for which the model is defined. The decay rate of the vacuum becomes then

$$\Gamma_{(2\ell)} \sim \left(\frac{\Lambda}{M}\right)^{8(\ell-1)} \frac{\Lambda^8}{M_{\mathrm{Pl}}^4} \quad (113)$$

$$\sim \left(\frac{t}{t_0}\right)^{4m(\ell-1)/(2m-1)} \left(\frac{\Lambda}{\mathcal{M}}\right)^{8(\ell-1)} \frac{\Lambda^8}{M_{\mathrm{Pl}}^4} \quad (114)$$

which depends on the time when the photons are created through $M(t)$. Denoting by $n_{(2\ell)}$ the number of photons created by vacuum decays, it satisfies a balance equation given by

$$\frac{d(a^3 n_{(2\ell)})}{dt} = a^3 \Gamma_{(2\ell)}, \quad (115)$$

which specifies how many photons accumulated since the very early Universe. The production is dominated by late times when $a^3 \Gamma_{(2\ell)}$ grows with time or decreases more slowly than $1/t$, which is the current case. Then, the number of photons today is set by the production at low redshifts with

$$t = t_0 : \quad n_{(2\ell)} \sim \frac{\Gamma_{(2\ell)}(t_0)}{H_0} \sim \left(\frac{\Lambda}{\mathcal{M}}\right)^{8(\ell-1)} \frac{\Lambda^8}{M_{\mathrm{Pl}}^4 H_0}. \quad (116)$$

The cutoff Λ should be above the scale $\mathcal{M}$, which sets the late time cosmological behavior associated with the dark energy era. Therefore, the highest production rate is governed by the highest order operator, $\ell = m$. The production is essentially occurring for $z \lesssim 1$ and is peaked at energies $E \sim \Lambda$ corresponding to an estimated spectrum

$$\frac{dF}{dE} \sim \frac{\Gamma_0}{\Lambda H_0}, \quad \text{with} \quad E \sim \Lambda, \quad \Gamma_0 = \left(\frac{\Lambda}{\mathcal{M}}\right)^{8(m-1)} \frac{\Lambda^8}{M_{\mathrm{Pl}}^4}. \quad (117)$$

This must be compared with the EGRET spectrum

$$\frac{dF}{dE} = 7.3 \ 10^{-9} \left(\frac{E}{E_0}\right)^{-2.1} \ (\mathrm{cm}^2.\mathrm{s}.\mathrm{MeV}.\mathrm{st})^{-1} \quad (118)$$

for $E \leq E_0 = 451$ MeV [28]. Imposing that the vacuum creates fewer photons than the observed ones for $E \sim \Lambda$, we get a bound on $\mathcal{M}$ which depends on m. Typically we find $\Lambda \leq 1$ keV for $m = 2$ and $\Lambda \leq 4$ eV for $m = 3$, and $\Lambda \to \mathcal{M}$ as $m \gg 1$. Consequently, the theories with ghosts (34) can only describe the very low energy physics

of the late acceleration of the Universe and cannot be considered as valid descriptions of physics since BBN. As a result, these theories seem to be very contrived and are less motivated than the ghost-free K-mouflage models (34), with $K_0 > 0$, and (35). Indeed, the kinetic function (35) contains a term $-\chi^2$ with a ghostlike negative sign. However, this does not give rise to the ghost instability discussed above because during the cosmological evolution we have $\bar{\chi} > \chi_*$, and we can check that $\bar{K}'$ and $\bar{K}''$ are positive, so that the quadratic term (105) has the standard positive sign.

Here we have made a perturbative analysis around the cosmological background $\bar{\varphi}$. This is legitimate because we impose the gamma ray constraint (118) before the creation of the field fluctuations $\delta\varphi$ overcomes the background. Indeed, at the redshifts of interest, $z \lesssim 2$, the scalar field energy density is of the order of the critical density, $\bar{\rho}_\varphi \sim \bar{\rho}_c$. The nonperturbative regime corresponds to $|\rho_{\delta\varphi}| \sim \bar{\rho}_\varphi$, which implies $\rho_\gamma \sim \bar{\rho}_c$ because the energy that goes into the generated photons is the opposite of the one that disappears in the ghosts. The upper bound $\rho_\gamma \lesssim \bar{\rho}_c$ is much looser than the EGRET constraint; therefore, we first reach the upper bound (118), far in the perturbative regime. This validates our perturbative analysis and the conclusions that theories with ghosts only make sense at very low energy.

VIII. CONCLUSION

We have presented a cosmological analysis of K-mouflage models, one of the three types of theories with screening properties for a long range scalar interaction on cosmological scales. In this paper, we have focused on the background cosmology. K-mouflage models are characterized by a nonlinear Lagrangian in the kinetic terms of a scalar field. In dense environments, such as the early Universe, the effects of the scalar field are screened and deviations from the Einstein-de Sitter cosmology characterizing the matter-dominated era become negligible. At late time, the background cosmology for small redshifts can be taken to be close to the one of an accelerated universe with a cosmological constant. In between these two epochs, the cosmology of K-mouflage models is rich and differs from the ones of chameleonlike and Galileon models, the other two archetypical models with screening properties. More precisely, in the early Universe, the screening of the scalar field does not imply that the dark sector of the model converges to the Λ-CDM model. Indeed, the equation of state of the scalar field converges in the far past to a negative constant, which is not equal to -1. At late time and for $z \lesssim 1$, the equation of state is not constant and can evolve by a few percent while other constraints such as the absence of disruption for Big Bang Nucleosynthesis are applied. For moderate redshifts, $1 \lesssim z \lesssim 5$, the Hubble rate is significantly different from the Λ-CDM case. Moreover, in the case where no quantum ghosts and therefore no vacuum instability are present, the equation of state always crosses the phantom divide and even diverges for moderate redshifts. This follows from the change of sign of the effective energy density of the scalar field which goes from negative in the distant past to positive in the recent past. The fact that the scalar energy density becomes negative does not jeopardize the soundness of the models, indeed the scalar becomes more and more screened in the past and the total energy density is always positive.

At the background level and for small redshifts, the K-mouflage models could be tested by observations of the time evolution of the equation of state. At the perturbation level, and as shown in a companion paper [17], the K-mouflage models are such that large-scale structures are still in the linear regime of the scalar sector. Therefore, deviations from Λ-CDM on the growth of large-scale structure and on the Integrated Sachs Wolfe effects are present. K-mouflage models are also very different from models like Galileons in the small-scale and large-density regime. The study of the behavior of K-mouflage models in this nonlinear regime is left for future work.

[1] E. J. Copeland, M. Sami, and S. Tsujikawa, Int.J.Mod.Phys. **D15**, 1753 (2006), hep-th/0603057.
[2] J. Khoury (2010), 1011.5909.
[3] L. Amendola et al. (Euclid Theory Working Group), Living Rev.Rel. **16**, 6 (2013), 1206.1225.
[4] C. de Rham, Comptes Rendus Physique **13**, 666 (2012), 1204.5492.
[5] C. Will, Pramana **63**, 731 (2004).
[6] P. Brax (2012), 1211.5237.
[7] P. Brax, Class.Quant.Grav. **30**, 214005 (2013).
[8] E. Babichev, C. Deffayet, and R. Ziour, Int.J.Mod.Phys. **D18**, 2147 (2009), 0905.2943.
[9] P. Brax, C. Burrage, and A.-C. Davis, JCAP **1301**, 020 (2013), 1209.1293.
[10] C. Armendáriz-Picón, T. Damour, and V. Mukhanov, Physics Letters B **458**, 209 (1999), hep-th/9904075.
[11] J. M. Cline, S. Jeon, and G. D. Moore, Phys.Rev. **D70**, 043543 (2004), hep-ph/0311312.
[12] J. Khoury and A. Weltman, Phys.Rev.Lett. **93**, 171104 (2004), astro-ph/0309300.

[13] J. Khoury and A. Weltman, Phys. Rev. **D69**, 044026 (2004), astro-ph/0309411.

[14] T. Damour and A. M. Polyakov, Nucl. Phys. **B423**, 532 (1994), hep-th/9401069.

[15] A. Vainshtein, Phys.Lett. **B39**, 393 (1972).

[16] E. Babichev, C. Deffayet, and G. Esposito-Farese, Phys.Rev. **D84**, 061502 (2011), 1106.2538.

[17] P. Brax and P. Valageas, ArXiv e-prints (2014), 1403.5424.

[18] J.-P. Uzan, Living Rev.Rel. **14**, 2 (2011), 1009.5514.

[19] P. Brax, C. van de Bruck, A.-C. Davis, J. Khoury, and A. Weltman, Phys. Rev. **D70**, 123518 (2004), astro-ph/0408415.

[20] B. Li, A. Barreira, C. M. Baugh, W. A. Hellwing, K. Koyama, et al., JCAP **1311**, 012 (2013), 1308.3491.

[21] A. Barreira, B. Li, W. A. Hellwing, C. M. Baugh, and S. Pascoli (2013), 1306.3219.

[22] J. Khoury (2013), 1312.2006.

[23] E. Babichev, C. Deffayet, and G. Esposito-Farese, Phys.Rev.Lett. **107**, 251102 (2011), 1107.1569.

[24] P. Brax and P. Valageas, Phys. Rev. D **86**, 063512 (2012), 1205.6583.

[25] P. Brax and P. Valageas, Phys. Rev. D **88**, 023527 (2013), 1305.5647.

[26] Planck Collaboration, P. A. R. Ade, N. Aghanim, C. Armitage-Caplan, M. Arnaud, M. Ashdown, F. Atrio-Barandela, J. Aumont, C. Baccigalupi, A. J. Banday, et al., ArXiv e-prints (2013), 1303.5076.

[27] W. Hu and I. Sawicki, Phys.Rev. **D76**, 064004 (2007), 0705.1158.

[28] P. Sreekumar et al. (EGRET Collaboration), Astrophys.J. **494**, 523 (1998), astro-ph/9709257.

[29] This potential can be obtained by going to the Jordan frame where test particles interact with the Jordan metric. In the Jordan frame, there is a second Newtonian potential $\Phi = \Psi_{\rm N} - \beta(\varphi_0)\frac{\delta\varphi}{M_{\rm Pl}}$. Notice that $\Phi + \Psi = 2\Psi_{\rm N}$ implying that the scalar field has no direct effect on lensing and only acts on the geodesics through Ψ.